SOME ASPECTS OF R-F PHASE CONTROL IN MICROWAVE OSCILLATORS

E. E. DAVID, JR.

TECHNICAL REPORT NO. 100

JUNE 11, 1949

RESEARCH LABORATORY OF ELECTRONICS
MASSACHUSETTS INSTITUTE OF TECHNOLOGY

The research reported in this document was made possible through support extended the Massachusetts Institute of Technology, Research Laboratory of Electronics, jointly by the Army Signal Corps, the Navy Department (Office of Naval Research) and the Air Force (Air Materiel Command), under Signal Corps Contract No. W36-039-sc-32037, Project No. 102B; Department of the Army Project No. 3-99-10-022.

MASSACHUSETTS INSTITUTE OF TECHNOLOGY

Research Laboratory of Electronics

Technical Report No. 100

June 11, 1949

SOME ASPECTS OF R-F PHASE CONTROL IN MICROWAVE OSCILLATORS

E. E. David, Jr.

ABSTRACT

Part I of this report describes phase modulation of a synchronized oscillator caused by changes in its d-c operating conditions. The effect of varying accelerator and reflector voltages of reflex klystrons and of anode voltage of magnetrons is discussed in detail. A general approach, applicable to any oscillator, is outlined, and a brief discussion of this type of modulation as a possible carrier of information is included.

When a magnetron is started in the presence of an external locking signal, transient effects which cannot be properly described by the steady-state equations take place. Part II of this report contains the derivation and solution of a differential equation which describes the phase of such a magnetron as a function of time. The initial conditions are established in terms of the locking signal-to-preoscillation noise ratio.

Pertinent reference material is included in the appendices.

SOME ASPECTS OF R-F PHASE CONTROL IN MICROWAVE OSCILLATORS

I. Introduction

In some electronic transmitters it is desirable to establish coherence between the transmitter oscillations and some reference signal whose frequency is not greatly different from that of the transmitter. It is often proposed to achieve this end by injection of energy from the reference source into the transmitter circuit. Provided that certain amplitude and frequency conditions are satisfied, the non-linear characteristics of the transmitter cause it to synchronize and, therefore, to become coherent with the reference signal.

This phenomenon has recently taken on new importance because of the rapid development, since 1940, of high-power microwave oscillators. It is now possible to generate kilowatts of power at frequencies as high as 30,000 Mc/sec. Similar rapid advances in methods of amplification, modulation, and frequency and phase control, however, have not been forthcoming. The synchronization phenomenon presents possibilities for accomplishing each of these functions. It is considered desirable, therefore, to investigate, both experimentally and theoretically, some of the more subtle aspects of this little-discussed field.

When the oscillations to be synchronized are of the continuous-wave type, the exact relation between synchronizing parameters and transmitter variables may be described in terms of the transmitter Rieke diagram, if the transmitter d-c conditions are fixed. This procedure has been described in detail (1). The results of such an analysis are equally applicable to pulsed transmitters, providing only that the pulse duration is long compared to the phase transient set up by the starting of the oscillator. It has been shown further that, when fixed transmitter d-c conditions are assumed and the synchronizing signal has specified power, frequency, and phase, the transmitter power, frequency, and phase are uniquely determined.* When operating in this condition, it is found that the transmitter phase is a function of the quantity $\omega_1 - \omega'$, where ω_1 is the frequency of the locking signal, and ω' is the transmitter frequency in the absence of the locking signal. Now ω' is a function of the transmitter d-c operating conditions, and therefore becomes time-variant if the supply voltages are modulated by noise. In such a case, the locking phase becomes similarly modulated. The first part of this report is concerned with an analytical and experimental examination of this effect. There is included a short discussion of its possible use as a device for communication of information.

* Synchronization in general, and this conclusion in particular, has been discussed by several authors. Some of these are listed in the bibliography.

When the oscillator to be synchronized is pulsed, there are present (attendant to the starting disturbance) certain transient conditions, which cannot be properly described by the usual steady-state theory. In particular, one would like to know the effect of preoscillation noise and the approximate duration and form of the phase and frequency transients. A differential equation characterizing the transient condition has been set up. Its derivation and solution are presented and discussed in the second part of the report.

Pertinent reference material is presented briefly in the Appendices.

II. Phase Modulation of Synchronized Oscillators

It has been shown previously (1) that when an oscillator is operating in a synchronized condition under the influence of a buffered, externally-applied, sinusoidal signal, the difference in phase between that signal and the generated oscillations is approximately

$$\phi = \sin^{-1}\left[\frac{Q_{ext}\,(\omega_1 - \omega')}{|\rho|\,\omega_o}\right] \qquad (1)^*$$

where ϕ is the phase difference

ρ is the reflection factor and is related to the reflection coefficient

ω' is the free-running oscillator frequency in the absence of the external signal

ω_1 is the frequency of the locking signal (assumed to be the same as that of the oscillator in the presence of the external signal)

ω_o is the natural frequency of the oscillator circuit

and Q_{ext} is a coupling factor.

If the synchronizing signal magnitude and frequency are independent of time, it is seen that the locking phase, ϕ, is a function of the free-running frequency only.** Now if this frequency is time-variant, the locking phase ϕ and, therefore, the oscillator phase will be time-modulated. The magnitude of this effect for a fixed variation of ω' is, of course, dependent on the relative powers of the synchronizing signal and oscillator output. The factor $|\rho|$ (proportional to the square-root of the ratio of these powers) in Eq. (1) shows the manner of this dependence.

---

* Equation (1) is derived and the constants involved are evaluated and discussed in Appendix I.

** The assumption of a constant-frequency locking signal does not affect the generality of this analysis since, so far as the locking phase is concerned, a change in ω_1 is equivalent to an equal negative change of ω'.

Now both the electronic conductance, g, and susceptance, b, as well as the r-f voltage, are functions of the d-c operating conditions of the oscillator. In general, if either or all of these three parameters change, both ω' and the power output are modified. If changes of the d-c conditions are not large, only the modification of ω' affects the locking phase appreciably. Accordingly, in this analysis variations of $|\rho|$ due to changes in the oscillator power output will be neglected, and the effect of d-c changes will be approximated by appropriate changes in ω' only.

In terms of the oscillator Rieke diagram this assumption states that small changes in the CRP or DL* contours in radial position resulting from changes in $|\rho|$ do not appreciably affect the angular position of the frequency contour intersections. Quite positively the larger effect is the shift of the frequency contours in angular position which accompanies variations in ω'. Assuming that a $\Delta\Phi$ results from a $\Delta\omega'$, we may write from Eq. (1)

$$\sin(\Phi + \Delta\Phi) = \frac{Q_{ext}\,(\omega_1 - \omega' - \Delta\omega')}{|\rho|\,\omega_o} \quad . \tag{2}$$

Writing an expression for $\sin\Phi$ from Eq. (1) and subtracting, we have

$$\cos\left(\Phi + \frac{\Delta\Phi}{2}\right) \sin\frac{\Delta\Phi}{2} = \frac{Q_{ext}}{2|\rho|\,\omega_o}\,\Delta\omega' \quad . \tag{3}$$

If $\Delta\Phi/2$ is small, this may be written

$$\Delta\Phi = 2\,\sin^{-1}\,\frac{Q_{ext}\,\Delta\omega'}{2|\rho|\,\omega_o\,\cos\Phi} \quad . \tag{4}$$

It is interesting to note that the phase deviation, $\Delta\Phi$, is a function of Φ itself. Also, from Eq. (1), it is seen that the maximum possible value of $|\omega - \omega'|$ occurs when $|\sin\Phi| = 1$, so for this limiting condition

$$(\omega - \omega') = \pm\,\frac{|\rho|\,\omega_o}{Q_{ext}} \tag{5}$$

and, of course, $\Phi = \pm\,\pi/2$. Near the edge of the locking band it is seen from Eq. (4) that the phase deviations approach quite large values even though $\Delta\omega'$ be small. The minimum of $\Delta\Phi$ is, of course, at the center of the locking band where $\Phi = 0$ and $\omega_1 - \omega' = 0$. Also, since $|\rho|$ is proportional to the square root of the synchronizing power, increases of this power are relatively ineffective in reducing $\Delta\Phi$. These conclusions will be discussed further in a later section.

So far we have spoken only of how variations of ω' affect the locking

---

* Constant reflected-power (CRP) and/or dynamic-load contours are the loci of operating points of the locked oscillator on its Rieke diagram. The locking phase is determined by the intersection between these and the constant-frequency contours (1).

phase, and have not discussed how the magnitude of these changes are related to the d-c operating conditions. In order to find these relations, it is necessary to know ω' as a function of these conditions. Although this functional relationship is known for some oscillators, it is quite difficult to obtain generally because of the inherent non-linear character of electronic discharges. However, experimental evidence may be used to provide a satisfactory picture in the more difficult cases.

III. Application to the Reflex Klystron and Magnetron

The reflex klystron presents a simple example in which the electronic relations may be derived analytically. The expressions for electronic conductance and susceptance as found by Slater ((2) p. 497) are

$$g = \frac{I_o}{V_o}\frac{\theta}{2}\cos(\theta - \tfrac{3\pi}{2})\frac{J_1(Z)}{Z}$$

$$b = \frac{I_o}{V_o}\frac{\theta}{2}\sin(\theta - \tfrac{3\pi}{2})\frac{J_1(Z)}{Z} \qquad (6)$$

where θ is the average transit angle of an electron in the reflector field and $J_1(Z)$ is the Bessel function of order one. (The remaining symbols are defined in Fig. 1.) It is seen that

$$b = -g\tan(\theta - \tfrac{3\pi}{2}) \quad . \qquad (7)$$

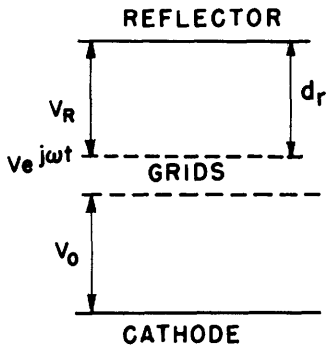

Fig. 1 Voltage definitions used in the derivation of reflex klystron equations.

d_r = reflector spacing
V_R = reflector voltage
V = r-f voltage
V_o = accelerator voltage
$Z = \frac{\theta}{2}\frac{V}{V_o}$

Now the output frequency of an oscillator is related to b by

$$\frac{b}{\omega_o C} = \frac{2(\omega' - \omega_o)}{\omega_o} + \frac{B}{Q_{ext}} \qquad (8)$$

where B is the normalized load susceptance. Combining Eq. (7) and Eq. (8),

$$-\frac{g}{\omega_o C}\tan(\theta - \tfrac{3\pi}{2}) = \frac{2(\omega' - \omega_o)}{\omega_o} + \frac{B}{Q_{ext}} \quad . \qquad (9)$$

But from the oscillator operating equation (1) we have ((2) p. 489)

$$\frac{g}{\omega_o C} = \frac{1}{Q_o} + \frac{G}{Q_{ext}}$$

where G is the normalized load conductance. So Eq. (9) becomes

$$\frac{2(\omega' - \omega_o)}{\omega_o} = \frac{B}{Q_{ext}} - \left(\frac{1}{Q_L} - \frac{1 - G}{Q_{ext}}\right) \tan\left(\theta - \frac{3\pi}{2}\right) \qquad (10)$$

where

$$\frac{1}{Q_L} = \frac{1}{Q_o} + \frac{1}{Q_{ext}} \quad .$$

Now the transit angle θ is

$$\theta = 2\sqrt{\frac{2md_r^2}{e}} \frac{\omega' V_o^{1/2}}{V_R} \qquad (11)$$

where m/e is the electronic mass-charge ratio. In this expression, ω' may be considered a constant since its percentage change is quite small compared to percentage variations in either accelerator or reflector voltages. Equations (10) and (11) then express ω' as a function of d-c voltages (and, of course, of the r-f load and oscillator design parameters). Together with Eq. (1) they may be used to express the locking angle ϕ in terms of V_o and V_r. After simplification, this expression is

$$\sin\phi = \left(\frac{Q_{ext}(\omega_1 - \omega_o)}{|\rho|\omega_o} - \frac{B}{2|\rho|}\right) + \left(\frac{Q_{ext}}{2|\rho|Q_L} - \frac{1 - G}{2|\rho|}\right) \tan\left(\zeta_1 \frac{V_o^{1/2}}{V_R} - \frac{3\pi}{2}\right) \qquad (12)$$

where

$$\zeta_1 = 2\sqrt{\frac{2m}{e}}\, d_r \omega' \quad .$$

It is possible to develop this equation further and find an expression for $\Delta\phi$ as a function of ΔV_o or ΔV_R, analogous to Eq. (4). Since such an expression contains no more information than Eqs. (4), (10), and (11), it will be omitted here.

It is possible to verify the above theory by a simple experiment. Suppose we allow the klystron reflector voltage to be modulated in a manner such that

$$V_R = V_{Ro}(1 + m \sin\omega_m t) \qquad (13)$$

where $\omega_m \ll \omega'$ then θ becomes approximately

$$\theta \simeq \zeta(1 - m \sin\omega_m t) \qquad (14)$$

where

$$\zeta = \zeta_1 V_o^{1/2}/V_{Ro} \quad ,$$

and assuming $m \ll 1$. Further, if the oscillator is operating at the center

of one of its modes into a matched load (that is, mismatched only due to locking signal),

$$\zeta = 2\pi n + \frac{3\pi}{2} \quad \text{and} \quad \left.\begin{matrix} G = 1 \\ B = 0 \end{matrix}\right\} \tag{15}$$

where n is the number of the operating mode. Then Eq. (12) becomes

$$\sin\phi = \frac{Q_{ext}\,(\omega_1 - \omega_o)}{|\rho|\,\omega_o} - \frac{Q_{ext}}{2|\rho|\,Q_L}\, m\zeta\, \sin\omega_m t \tag{16}$$

so long as $m\zeta < 30°$. Here ρ is the reflection coefficient. This equation may be used to describe the circuit shown in Fig. 2 where a stabilized source supplies a small buffered locking signal to a 707-B klystron through a two-way matched attenuator. A spectrum analyzer is used in conjunction

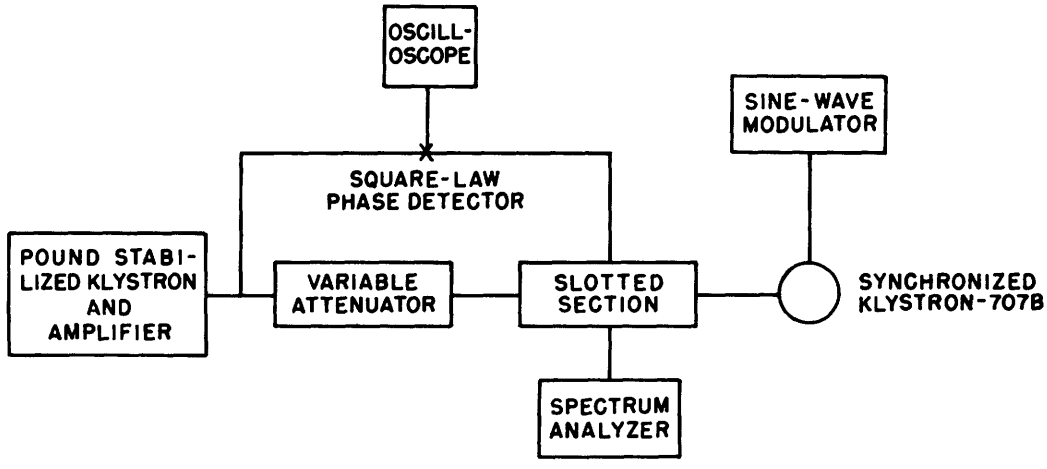

Fig. 2 A circuit which can be used to examine the relative phase of a locked oscillator.

with the slotted section to measure the reflection coefficient presented to the 707-B. The 707-B and stabilized outputs are sampled by suitable probes which feed a phase-sensitive, square-law detector. The reflector voltage of the 707-B is sinusoidally modulated by a variable amplitude signal.

When the 707-B is locked, the detector input is

$$V_{in} = V_{stab}\cos\omega t + V_{707}\cos(\omega t + \phi) \quad . \tag{17}$$

The detector output is the square of the vector sum of the magnitudes,

$$V_{out} = V_{stab}^2 + V_{707}^2 + 2V_{stab}V_{707}\cos\phi \quad . \tag{18}$$

If we write $\phi = \phi_o + \phi(t)$, we see that the oscilloscope will give an indication proportional to $\cos[\phi_o + \phi(t)] = \sin\phi(t)$ if $\phi_o = \pi/2$. In our experimental circuit ϕ_o may be adjusted merely by shifting the pick-up probe

position. When the synchronizing frequency ω is made equal to the 707-B cavity resonant frequency ω_o, the detector output is proportional to the time-varying term in Eq. (16). That is,

$$\sin\Phi = -\frac{Q_{ext}}{2|\rho|Q_L} m\zeta \sin\omega_m t \quad . \tag{19}$$

Here Φ has a real value only when the right-hand side of the equation is less than 1. It is quite possible that m, the modulation index, will be large enough so that this condition is not satisfied on the modulation peaks. This indicates merely that $|\omega - \omega'|$ is so large at these points that locking is no longer maintained. Figure 3 shows a phase pattern of this

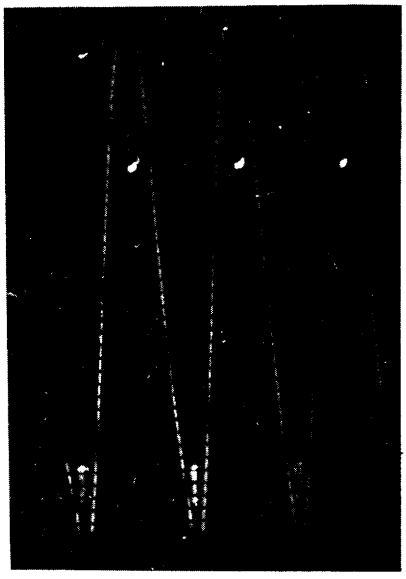

Fig. 3 Variation of $\sin\Phi$ when a locked klystron is reflector-modulated with a 60-cycle sinusoidal voltage. Note the break in synchronism on the modulation peaks.

type. The sharp breaks at the sine-wave peaks indicate the unsynchronized portion of the cycle.

Equation (19) may be examined experimentally in order to verify partially the above theory. Figure 4 shows how the maximum value of $\sin\Phi$ varies with reflection coefficient if all other parameters are held constant. The reflection coefficient was measured with the modulation voltage removed. The experimental points show close agreement with the theoretical curves as found from Eq. (19). Note that no experimental points are available for reflection coefficients less than .13 since at this point the coefficient of $\sin\omega_m t$ in Eq. (19) had become equal to unity, and synchronism at the peaks of the modulation cycle was no longer possible. At this boundary

$$\frac{|\rho|}{m} = \frac{Q_{ext}}{2Q_L}\zeta \quad . \tag{20}$$

This relation may be used to provide a quantitative check of Eq. (19). By

cold test the ratio of Q's may be found, and ζ is merely the steady-state value of the transit angle, θ. These values were found to be

$$\frac{Q_{ext}}{2Q_L} = 6.7 \quad \text{and} \quad \zeta = 4\pi + \frac{3\pi}{2} = 17.3 \text{ radians.}$$

Therefore,

$$\frac{Q_{ext}}{2Q_L}\zeta = \frac{6.7}{2} \times 17.3 = 58 \quad .$$

At the locking boundary in Fig. 4

$$\frac{|\rho|}{m} = \frac{.13}{.6}\, 229 = 50 \quad .$$

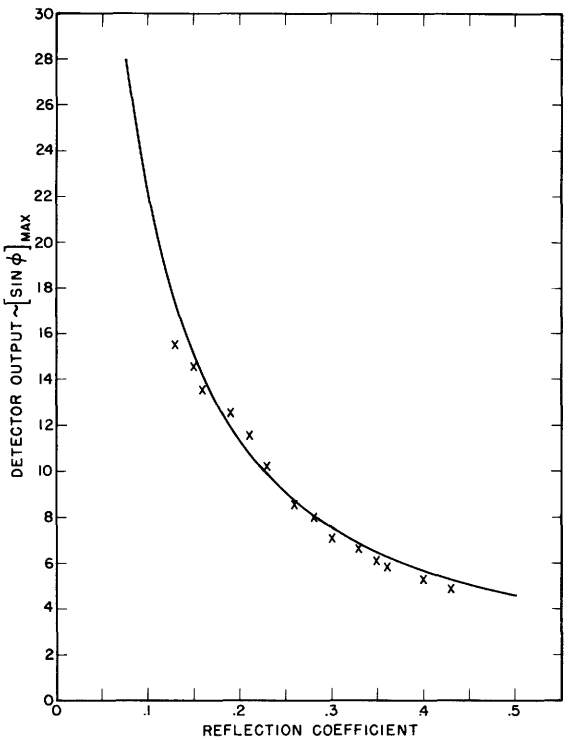

Fig. 4 Variation of the maximum of sinϕ with reflection coefficient.

——— = theoretical curve
x = experimental point
reflector modulation = 0.6 v
reflector voltage = 229 v
klystron n = 2 mode
klystron power out = 60 Mw

Spot checks at other values of m give the $|\rho|/m$ ratio values ranging from 50 to 70. These results fall within the theoretical limitations of the analysis.

Equation (19) shows that maximum variations of sinϕ will be directly proportional to the modulating voltage. Experimentally this was found to be the case as is shown in Fig. 5. Note that this modulation characteristic intersects the voltage axis to the left of the origin. We may deduce, therefore, that the phase is modulated by hum from the power supply. This hum is present in varying amounts on all klystron electrodes. Figure 5 shows that it is equivalent to a reflector modulation of about 0.1 volt. The effects of this small voltage are quite apparent when the synchronizing

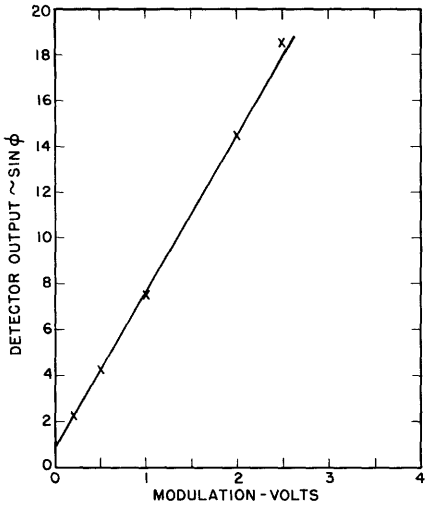

Fig. 5 Modulation characteristic.
$|\rho| = 0.2$
reflector volts = 229
x = experimental points.

a b

Fig. 6 (a) Phase modulation of a synchronized klystron by power supply hum when $|\rho| = 0.01$. Note that synchronism is not maintained on the negative modulation peaks. (b) Phase of same klystron when battery operated.

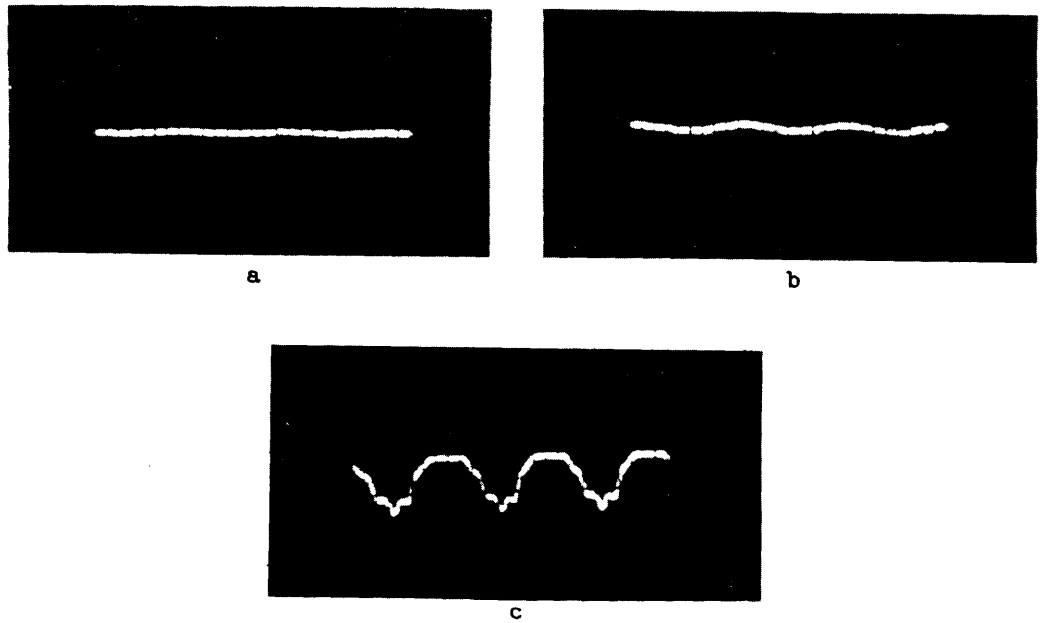

a b c

Fig. 7 (a) Phase of a locked klystron when $|\rho| = 0.01$. Both heater and reflector, but not anode, are battery supplied. (b) Reflector, but neither heater nor anode, battery supplied. (c) All electrodes operating from normal supplies.

power is small. Figure 6a shows the phase pattern when $|\rho| = 0.01$. It is to be compared to that in Fig. 6b, which is also for $|\rho| = 0.01$. However, all klystron electrodes are supplied by batteries. It was found that hum from the a-c heater had an appreciable effect on the phase, probably due to the action of the stray a-c field, but this modulation is small compared to that of the reflector ripple. The relative importance of these sources of noise may be compared in Fig. 7. These phase patterns show further that, in this instance, the effect of hum in the anode supply is negligible.*

These experimental results show our analysis to be sound, so that we may continue a more general discussion of the phase of a synchronized klystron. We choose to restrict the analysis to an oscillator operating near the center of one of its modes ($\theta = 2\pi n + 3\pi/2$), and one in which the percentage change in reflector voltage is small. As previously, the changes in anode voltage V_o will be neglected. From Eq. (14), it is seen that the extreme values of θ may be written as

$$\theta_{ext} = \zeta(1 \pm m) \tag{21}$$

where m is the maximum percentage change of V_R. Under the above assumptions, provided $m\zeta < 30°$, Eq. (12) becomes

$$\sin\phi_{ext} = \frac{\lambda}{|\rho|} \pm \frac{\gamma}{|\rho|} \tag{22}$$

where ϕ_{ext} = the extreme value of ϕ;

$\lambda = \frac{Q_{ext}}{\omega_o}(\omega_1 - \omega_o) - \frac{B}{2}$, a factor depending on the synchronizing frequency and giving the steady-state value of ϕ;

$\gamma = \left(\frac{Q_{ext}}{2Q_L} - \frac{1 - G}{2}\right)m\zeta$, the dimensionless modulating parameter;

and $|\rho|$ = the reflection factor, proportional to the square root of

---

* The effect of hum on the klystron anode has been neglected in this analysis for the sake of simplicity. However, this factor may be included without difficulty if an expression of the form of Eq. (13) is assumed for V_o and substituted into Eq. (12). There results from such a calculation

$$\sin\phi = \frac{Q_{ext}(\omega_1 - \omega_o)}{|\rho|\omega_o} - \frac{Q_{ext}}{2|\rho|Q_L} M_R\zeta \sin\omega_{M_R} t + \frac{Q_{ext}}{2|\rho|Q_L}\frac{M_o}{2}\zeta \sin\omega_{M_o} t$$

where

$$\omega_{M_R},\ M_R,\ \omega_{M_o},\ M_o$$

are respectively the modulation frequency and index on the reflector and anode. In the derivation, it has been assumed that M_r and M_o are small.

the synchronizing power, and reducing to the reflection coefficient when the passive load is matched.

Now we may write Eq. (22) as

$$\phi_{ext} = \sin^{-1}\left(\frac{\Psi}{|\rho|}\right) \qquad (23)$$

where $\Psi = \lambda \pm \gamma$. From this expression, we may plot the extreme value of ϕ as a function of $|\rho|$ with ψ as a parameter. This is done in Fig. 8 for positive values of Ψ. Note that the Ψ contours are even functions about the reflection factor axis. It is seen that the derivative $d\phi_{ext}/d|\rho|$

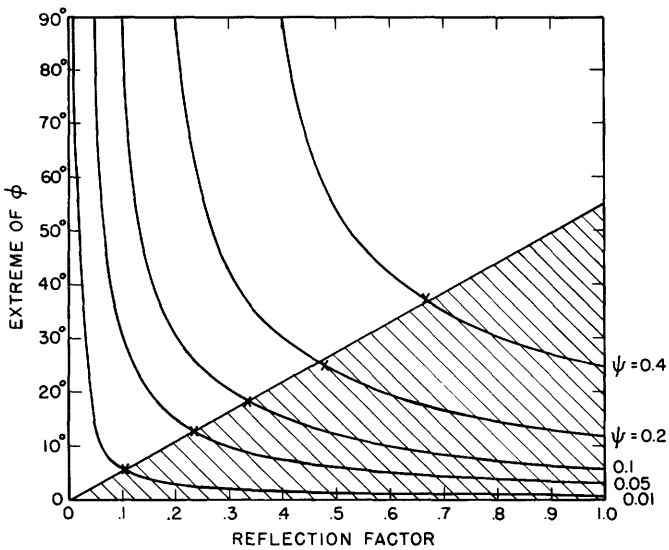

Fig. 8 Effect of reflection factor and the parameter, ψ, on the extreme value of the locking angle, ϕ. $\psi = \lambda \pm \gamma$

decreases sharply toward zero as $|\rho|$ increases. The physical interpretation of this fact may be seen by considering the case when $\lambda = 0$, $\gamma = 0.1$, and $|\rho| = 0.15$. In this condition, the oscillator has a phase deviation of about 41°. An increase of $|\rho|$ to 0.33 reduces this to 18°, a decrease of 23°. However, if our purpose is to minimize the phase deviations, further increase of $|\rho|$ is relatively ineffective in producing the desired result. In other words, if a small angular tolerance is desired, it should be achieved by decreasing Ψ rather than increasing the synchronizing power ($|\rho|$). The diagonal line in Fig. 8 is the locus of points at which the $d\phi_{ext}/d|\rho|$ derivative is 50° per unit-increase in $|\rho|$. It marks the approximate boundary between regions of efficient and inefficient operation.

Suppose that the system is operating at $|\rho| = 0.2$ and $\Psi = 0.05 \pm 0.05$. We see that the phase varies between zero and 30 degrees. If Ψ is increased

to 0.10 ± 0.05, the phase boundaries are 14° and 90°. It is seen that the phase deviation is a rapidly increasing function of λ, the constant part of Ψ. The minimum deviation, of course, occurs for $\lambda = 0$.

These are the same conclusions we have drawn for the general oscillator from Eq. 4. In this case, however, we have found a direct quantitative relation between phase and the modulating index, involving the locking parameters, load impedance, and klystron design characteristics. In the case of a more complex oscillator, such as the magnetron, it is not possible, at present, to obtain such a general result. However, it is possible to derive an expression which, when used in conjunction with experimental data, will be valuable in determining the behavior of the phase of any locked oscillator.

As has been noted previously, the phase change in a locked oscillator is dependent on the change in ω', the free oscillating frequency. Any change, $d\omega'$, may be expressed as

$$d\omega' = \frac{\partial\omega'}{\partial A_{dc}} dA_{dc} + \frac{\partial\omega'}{\partial B_{dc}} dB_{dc} + \ldots \qquad (24)$$

This relation is still valid if the changes in d-c variables are finite, but small. Equation (24) then becomes

$$\Delta\omega' = \frac{\partial\omega'}{A_{dc}} \Delta A_{dc} + \frac{\partial\omega'}{\partial B_{dc}} \Delta B_{dc} + \ldots \qquad (25)$$

Applying this relation to Eq. (4), we have

$$\phi = 2\sin^{-1}\left[\frac{Q_{ext}}{2|\rho|\omega_o \cos\phi}\left(\frac{\partial\omega'}{\partial A_{dc}} \Delta A_{dc} + \frac{\partial\omega'}{\partial B_{dc}} \Delta B_{dc} + \ldots\right)\right] \qquad (26)$$

The differential coefficients appearing here may be determined experimentally for the particular case. These coefficients, of course, are functions of the operating conditions of the oscillator. In general, these include d-c parameters and r-f load. One would say, therefore, that complete evaluation of the coefficients would be an arduous task, particularly if the d-c parameters were numerous; but if one wished to design an accurately phased system, a comprehensive study of these factors might prove valuable. In the more usual case, operating conditions are determined by requirements other than the phase tolerance, so that an extensive evaluation of these derivatives is unnecessary.

An analysis of the type described above has been carried out on a QK-61 magnetron oscillator for one value of magnetic field. The tube operated into a load whose conductance was variable, but whose susceptance was zero. For several values of conductance, the plate voltage-frequency relation was recorded. These data allow the partial derivative, $\partial\omega'/\partial V_{dc}$,

to be calculated. How this may be accomplished can be seen by considering the operating equations (1)

$$g/\omega_o C = 1/Q_o + G/Q_{ext} \qquad \text{and} \qquad b/\omega_o C = 2\left(\frac{\omega' - \omega_o}{\omega_o}\right) + B/Q_{ext} \,. \tag{27}$$

Let us normalize the electronic conductance to its value when the load is matched. Then

$$\mathcal{G} = \frac{g}{g_o} = \frac{1 + G\,Q_o/Q_{ext}}{1 + Q_o/Q_{ext}} \tag{28}$$

where $g_o = 1/Q_o + 1/Q_{ext} = 1/Q_{Lo}$ is the matched electronic conductance and $\mathcal{G}$ is the normalized electronic conductance. Similarly,

$$\mathcal{B} = \frac{b}{g_o} = 2Q_{Lo}\left(\frac{\omega' - \omega_o}{\omega_o}\right) + \frac{Q_{Lo}B}{Q_{ext}} \tag{29}$$

where $\mathcal{B}$ is the normalized electronic susceptance. From our measurements and the cold-test data on the QK-61, Eqs. (28) and (29) allow $\mathcal{G}$ and $\mathcal{B}$ to be calculated for B = 0. Now it is very closely true that, in a magnetron, changes of B effect only ω' and not $\mathcal{B}$. Therefore, our experimentally determined $\mathcal{B}$ may be used to find the value of the right-hand side of Eq. (29) for any B.

In Fig. 9, we have plotted

$$\frac{\mathcal{B}}{2Q_{Lo}} + 1 = \frac{\omega'}{\omega_o} + \frac{B}{2Q_{ext}}$$

as a function of $\mathcal{G}$ for various values of magnetron plate voltage.* Now the load conductance, G, determines the operating locus of the oscillator, which is merely a vertical line crossing the $\mathcal{G}$-axis at the appropriate value indicated by Eq. (28). For any plate voltage intersection of the locus, the desired derivative may be found. Fig. 10 shows the frequency parameter as a function of plate voltage for constant values of $\mathcal{G}$. The slope of these curves is $\partial\omega'/\partial V_{dc}$. These contours were taken directly from Fig. 9, although they could have been found directly from the original data. The value of such a plot is that it allows extrapolation of the data for any value of load conductance. The behavior of both sets of curves shows the interesting, but not unexpected, fact that electronic and r-f conductive loading of the oscillator increases its frequency sensitivity. An equivalent statement, of course, is that this loading lowers the effective oscillator Q, thereby reducing its frequency stability. The region of

* These measurements were originally made by R. R. Moats. They were later checked by the author.

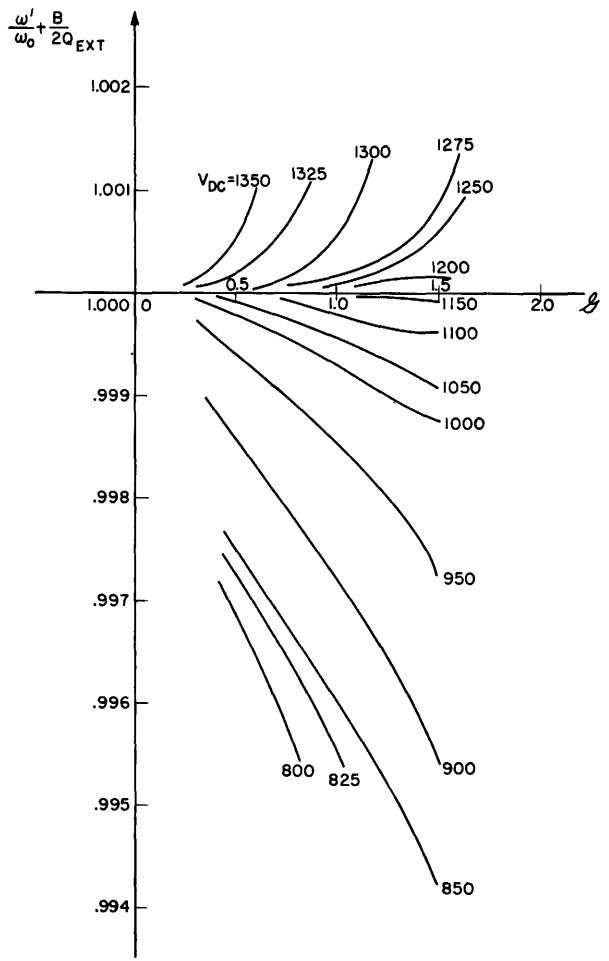

Fig. 9 Frequency characteristic of QK-61 magnetron as a function of electronic conductance.

B = 1700 gauss

f_o = 3185 Mc

Q_o = 1220

Q_{ext} = 310

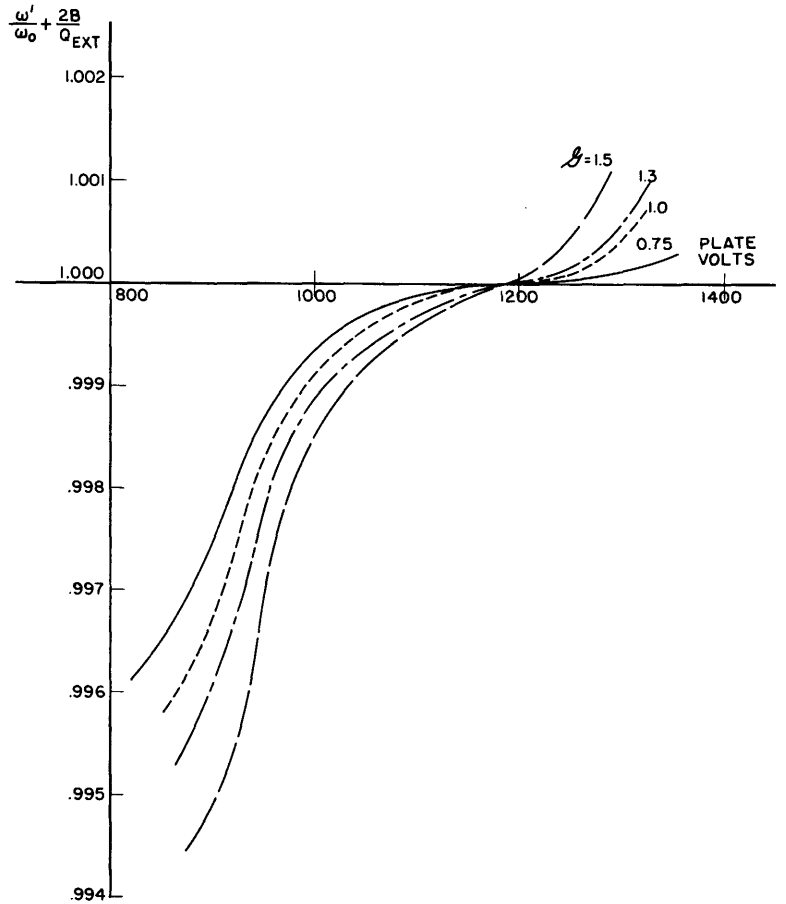

Fig. 10 Frequency characteristic of QK-61 magnetron as a function of plate voltage.

B = 1700 gauss

f_o = 3185 Mc

Q_o = 1220

Q_{ext} = 310

the greatest stability, independent of conductive loading, is around 1175 plate volts.

An experimental circuit used to synchronize the QK-61 magnetron is shown in Fig. 11. The synchronizing signal is again supplied by a Pound-

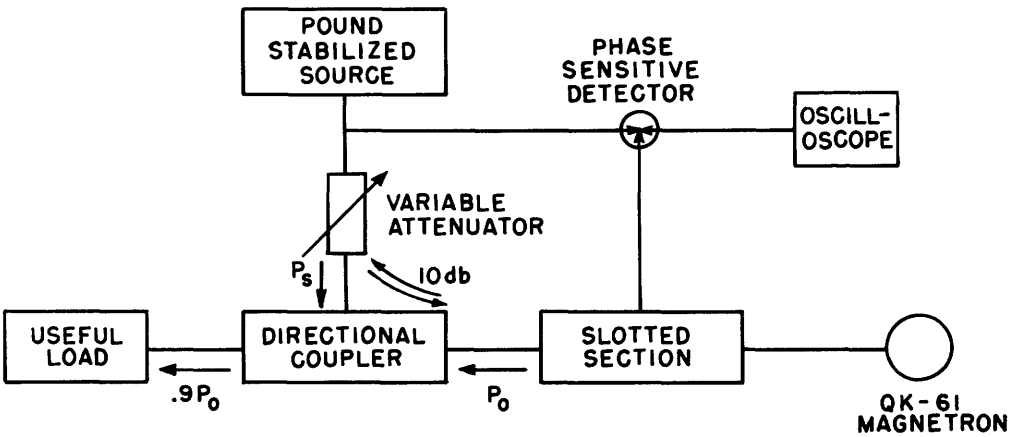

Fig. 11 A circuit that might be used in practical applications of the locking phenomena. This arrangement has been used in experiments with a synchronized magnetron.

stabilized klystron and amplifier whose maximum output power is about 6 watts. This magnitude may be adjusted by the variable attenuator. The locking signal is injected into the main oscillator line through a directional coupler whose loss is 10 db. This method of injection allows the entire locking power to propagate toward the QK-61 rather than being divided between it and the useful load. The magnetron output power suffers only a 0.5-db loss in transmission through the coupler on its way to the load. The arrangement has a high r-f efficiency, specifically

$$\eta_{rf} = \frac{0.9P_o}{P_o + P_s} \quad . \tag{30}$$

In this particular circuit, η_{rf} = 82 percent; the useful power is 54 watts; approximately 12 watts are lost in the directional coupler. The r-f power gain of the circuit is 9.5 db. Both the efficiency and the power gain could be increased at the expense of phase stability by decreasing the synchronizing power or increasing the coupler attenuation. An optimum compromise among these factors may be reached by use of practical considerations. Note that when no synchronizing power is applied, the magnetron operates into an approximately matched load.

Examination of the phase of the locked QK-61 reveals close agreement with behavior predicted from Eq. (26) and Figs. 9 and 10. A close quantitative check on the above theory is difficult to carry out since any

appreciable ripple on the magnetron plate results in severe amplitude modulation of the output. The phase indicator used in these experiments is amplitude sensitive, so that the two effects are inseparable in the present circuit.

Note that in all the previous derivations, the tacit assumption has been made that the modulation frequencies involved are low. That is, we have considered the period of any frequency component in the modulating wave long, compared to the duration of any transients in the system. Hence, our analysis is valid only when quasi-steady-state conditions exist. If this condition is not satisfied, one must solve the system differential equation in order to describe the phase correctly. These matters are discussed more fully in Section IV.

IV. Some Possibilities for Transmission of Information

Until the present, phase modulation of a synchronized oscillator by variations in its d-c operating conditions has been considered mainly a nuisance effect. It is apparent now, however, that this effect might be utilized for the transmission of information. No great amount of work has yet been done in this field and a thorough investigation of the possibilities might prove valuable. The discussion below is intended merely as a brief outline of some of the factors that would be involved in such an investigation.

In order to provide a symmetrical modulation characteristic, we must choose $\omega_1 - \omega'$ zero when no modulation voltage is applied. With sinusoidal modulation, the phase becomes

$$\sin\phi = \frac{W}{S}\sin\omega_m t$$

where $-\pi/2 \leqslant \phi \leqslant \pi/2$,

or
$$\phi = \sin^{-1}\left[\frac{W}{S}\sin\omega_m t\right] \qquad (31)$$

where $0 \leqslant W/S \leqslant 1$; $W = \left|(\omega_1 - \omega')_{max}\right|$, the maximum frequency deviation which is a function of the amplitude of the modulating voltage; and $S = |\rho|\omega_o/Q_{ext}$. It is seen that this is not the usual phase modulation; here, the sine of the phase, rather than the phase itself, is proportional to the modulating voltage. Therefore, the sidebands produced will differ from the more usual case. More specifically, consider a carrier $E_c \cos\omega_1 t$ modulated by our method. It then becomes

$$e(t) = E_c \cos(\omega_1 t + \Phi)$$

where $-\pi/2 \leqslant \Phi \leqslant \pi/2$

or
$$e(t) = E_c \cos\left\{\omega_1 t + \sin^{-1}\left[\frac{W}{S}\sin\omega_m t\right]\right\} \qquad (32)$$

where $0 \leqslant W/S \leqslant 1$. This expression shows immediately that the spectrum of this wave will be the same as that of a wave conventionally phase-modulated by a voltage proportional to $\sin^{-1}[W/S \sin\omega_m t]$. Therefore, there will be an infinite number of sidebands spaced at the harmonic frequencies of ω_m. In order to find the actual spectrum, it is necessary to expand $\sin^{-1}[W/S \sin\omega_m t]$ in a Fourier series, substitute into Eq. (32) and expand this by trignometric identities ((3) pp. 154-5). This tedious process will not be carried out here.

This phase modulation scheme might be used directly for communication purposes; and also to produce an ordinary amplitude-modulated wave. Consider two independent oscillators, tuned to the same frequency, locked to the same reference source, and push-pull modulated by a sine wave. If the r-f waves thereby produced are combined in the proper phase, the resultant shows the same characteristics as the sidebands of amplitude modulation. Just how this comes about is shown in Fig. 12. There it is assumed that the amplitude of the r-f waves are equal; the oscillators are identical; and the modulating voltage is a sinusoid, $V_m \sin\omega_m t$. It is seen that a wave proportional to the instantaneous modulating voltage is produced. It may be considered the sum of two equal waves of frequency $(\omega_1 + \omega_m)$ and $(\omega_1 - \omega_m)$. If a carrier is desired, power from the reference source may be added.

In addition to modulation of a locked oscillator by changes in its d-c operating conditions, variations of locking signal amplitude and frequency present potentialities for communication. We may draw the conclusion that the possibilities for modulation are numerous.

The above discussion makes the important assumption that the modulating frequency is low enough so that $d\Phi/dt$ is negligible compared to S. Consider the differential equation of the system, as derived in Appendix I, when sinusoidal modulation is applied. Equation (I-10) becomes

$$\frac{d\Phi}{dt} + S \sin\Phi = W \sin\omega_m t \quad . \qquad (33)$$

In order that Eq. (31) be a solution,

$$\frac{d\Phi}{dt} = \frac{\frac{W}{S}\omega_m \cos\omega_m t}{\left[1 + \left(\frac{W}{S}\sin\omega_m t\right)^2\right]^{1/2}} \ll S \quad \text{for all } t \quad . \qquad (34)$$

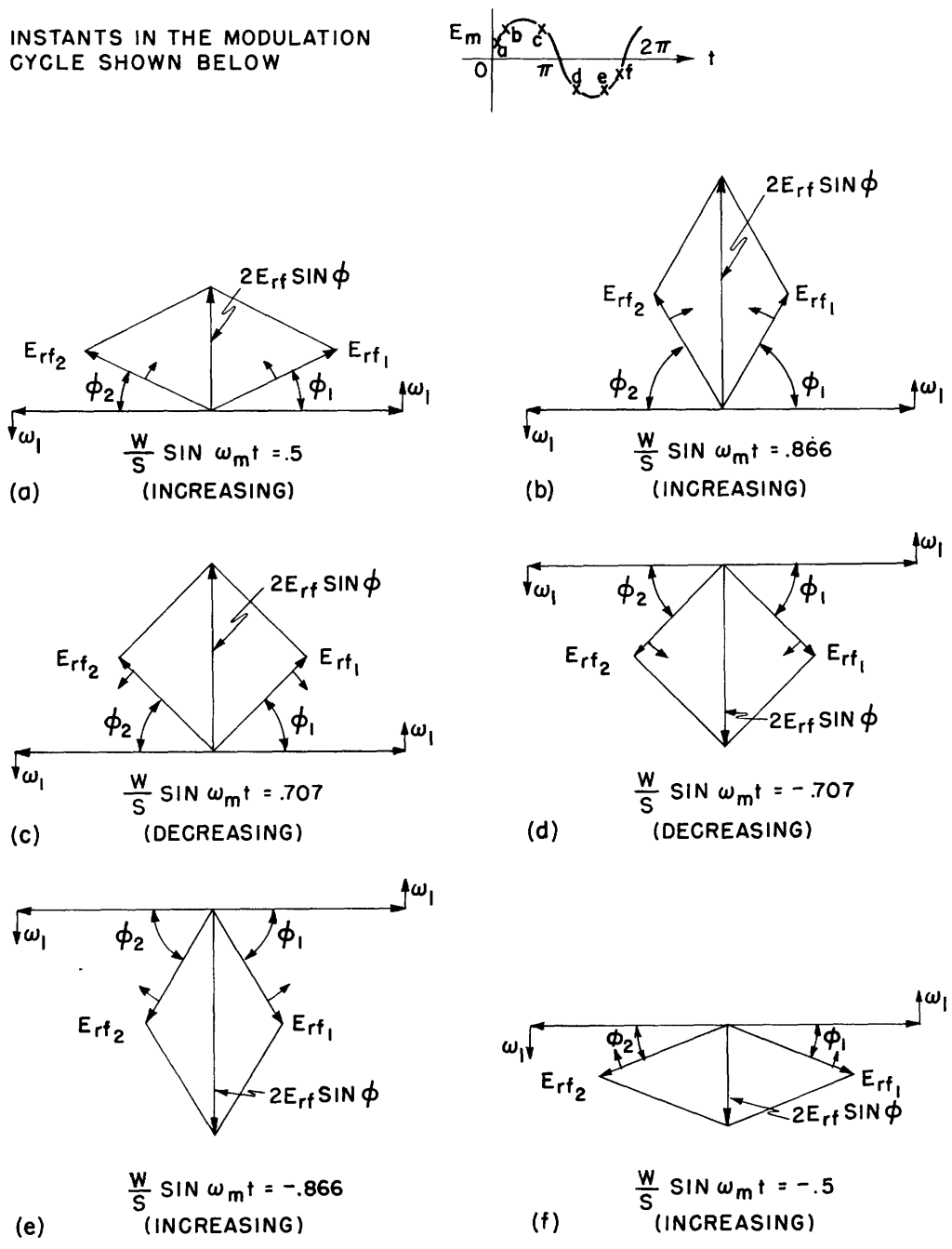

Fig. 12 Wave produced at successive instants of time by the addition of two phase-modulated signals. Note that each vector diagram is rotating at the reference angular frequency, ω_1.

$$v_m = V_m \sin\omega_m t$$

$$\Phi = \sin^{-1}(W/S \sin\omega_m t) \qquad -\pi/2 \leq \Phi \leq \pi/2$$

$$2E_{rf} \sin\Phi = (2E_{rf}\, W/S) \sin\omega_m t \qquad 0 \leq W/S \leq 1$$

where $E_{rf} = E_{rf_1} = E_{rf_2}$, and $\Phi = \Phi_1 = \Phi_2$

This is a relation which may be used to establish the useful modulation bandwidth.

There is another important consideration which should be pointed out here. We see from Eq. (33) that the system is inherently a non-linear one. Therefore, the usual superposition of Fourier components is not a valid procedure. To clarify this statement, consider that we have the explicit solution to Eq. (33) and have thereby established the sinusoidal frequency response of the phase. Now, unlike a linear system, this characteristic does not establish the response of the system to a transient voltage, f(t). To find this response, it is necessary to solve the equation

$$\frac{d\phi}{dt} + S \sin\phi = Wf(t) \quad . \tag{35}$$

Actually, very little can be said in general about the properties of the phase as a carrier of information. These matters must be fully investigated before any of the schemes discussed above can be used with a high degree of reliability. It does seem, however, that the possibilities are such as to warrant a close examination of the factors involved.

V. Description of Starting and Probable Character of Magnetron Preoscillation Noise

In many high-power microwave applications, the transmitter tube is operated with a short duty-cycle so that large peak power may be obtained with relatively low average input power. During successive pulses the phases of the oscillations bear no definite relationship. This condition is quite undesirable in some types of radar systems and may be remedied if the transmitter is synchronized by a continuous-wave signal. The conventional theory, which discusses the steady-state oscillator when influenced by a suddenly applied locking signal, is not adequate to describe the pulsed case. In particular, the effects of the starting transient must be accounted for. Therefore, we would like to find a differential equation in ϕ for the system, including these effects. Such an equation is derived in Section VII. It reduces to the former case (Eq. (I-10)) when the effects of the starting transient die out. This equation is applied specifically to the magnetron, since this is the tube most widely used in pulsed microwave applications. The derivation assumes that the starting is a succession of steady-states; that is, the analysis utilized the steady-state properties of the magnetron to describe the transient. This assumption will be discussed in Section VII.

The initial conditions on the starting equation may be established if we examine the state of the oscillator at the first instant of starting. Upon application of a step-function voltage to the plate of a magnetron,

electronic charge begins immediately to fill the interaction space. Initially the coupling between the incoherent space-charge and the resonant structure is small. The increase of this coupling with time is accompanied by build-up of noise voltage on the anode. This noise becomes a maximum just before coherent oscillations begin. When the conditions for oscillation are established, the electronic beam jumps almost discontinuously into a regenerative condition from which finite oscillations begin to build up. These oscillations spring from the voltage already present on the plate; in this case, the preoscillation noise. If there is an external sinusoidal signal impressed upon the magnetron, the initial oscillations start from the vector sum of this and the noise voltage. If the character of the preoscillation noise can be deduced, this sum may be used to establish the required initial conditions.

During the preoscillation time of the magnetron, the incoherent space-charge is inducing noise voltage on the anode. The spectrum of this voltage has an amplitude distribution that is determined by the sinusoidal cavity response. The situation is analogous to the case of a tuned circuit being driven by a current whose frequency spectrum is much wider than the bandwidth of the tank. The voltage response waveform to such a disturbance is practically independent of the exciting waveform and is almost completely defined by the tuned-circuit selectivity and sensitivity. In our case, a wide-band noise current is driving a high-Q resonant structure. Certain conclusions, therefore, may be drawn as to the character of the resulting voltage on the magnetron vanes.

First, the noise voltage bandwidth is that determined by the cavity Q. Approximately, therefore, the voltage is sinusoidal over $2\omega_o/10W$ r-f cycles, where ω_o is the cavity resonant frequency and W is the cavity bandwidth.* The average frequency of the sinusoid over a large number of r-f cycles is the resonant frequency; however, this signal is frequency-modulated in a random manner as indicated by the noise sidebands. Over a large number of cycles, then, its phase is likewise random in the interval 0 to 2π. Similarly, the noise envelope varies slowly in a random manner. It can be shown that the probability distribution of this envelope is approximately ((3) p. 336).

$$P(e_n)de_n = \frac{2e_n}{\overline{e_n^2}} e^{-e_n^2/\overline{e_n^2}} de_n \qquad (36)$$

* The bandwidth and resonant frequency referred to here are approximately those of the cold cavity since the electronic beam loading is small during the noise build-up.

where e_n is the noise envelope amplitude and $\overline{e_n^2}$ is the mean squared noise envelope amplitude. The above discussion is equivalent to the statement that the fine-grained noise structure is sinusoidal while the coarse-grained structure is that of random variations.

It is seen, therefore, that when no external voltage is impressed, the starting phase is completely random. In the presence of an external signal, the starting phase may be determined statistically from the relative signal and noise powers.

VI. Statistical Properties of the Phase of a Sine Wave plus Random Noise

It has been postulated that the magnetron preoscillation noise approximates a sine wave of random phase and statistical amplitude over a small number of r-f cycles. We are interested in the phase of the resultant magnetron voltage during a very short interval at the beginning of the starting period. This voltage, therefore, may be found by considering the sum of two vectors: one, of constant phase and fixed amplitude; the other of random phase and statistical amplitude. The statistical phase of the resultant may be deduced therefrom.

Now in an actual case of starting, the "mean noise frequency" may differ appreciably from the synchronizing frequency. Fortunately this difference is small in percentage and, since the noise phase is random, does not affect the validity of our representation. The randomness fixes the phase during any short period, and the phase shift due to the frequency difference is negligible during this interval.

Consider, then, the vector relationship shown in Fig. 13 where N is the noise voltage amplitude of phase ξ, C is the locking signal amplitude, and A is the resultant of phase Φ. Now A may be expressed as

$$Ae^{j\Phi} = C + N\cos\xi + jN\sin\xi \tag{37}$$

whose phase is

$$\Phi = \tan^{-1}\left(\frac{N\sin\xi}{C + N\cos\xi}\right) = \tan^{-1}\left(\frac{R\sin\xi}{1 + R\cos\xi}\right) \tag{38}$$

where $R = N/C$. Let us first find the statistical properties of Φ from those of ξ, considering R merely as a parameter. The probability of R may be superposed on this solution to obtain the desired result. Equation (38) shows that the initial part of our solution falls into two cases: Case I, $0 \leqslant R \leqslant 1$; and Case II, $1 < R < \infty$.

Case I

If $R < 1$, Φ always lies in either the first or fourth quadrant for any

value of ξ. More specifically, ϕ is a double-valued function of ξ, as seen from Eq. (38). For any finite sector, $d\phi$, there are two corresponding sectors $d\xi_1$ and $d\xi_2$. This is shown in Fig. 14. The probability of ϕ lying in

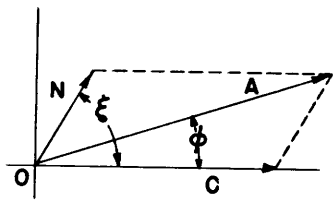

Fig. 13 Vector relationship of ϕ to the noise angle ξ.

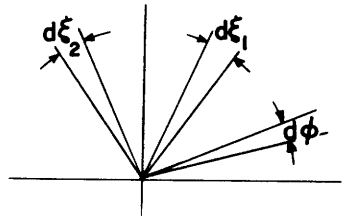

Fig. 14 Finite sector $d\phi$ with its corresponding sectors $d\xi$ and ξ_2.

the interval $d\phi$ is the sum of the probabilities of ξ lying in the intervals $d\xi_1$ and $d\xi_2$. That is,

$$P(\phi,R)d\theta = P(\xi)\,[|d\xi_1| + |d\xi_2|] \tag{39}$$

where $P(\xi) = \frac{1}{2\pi}$, since we have assumed ξ to be random in the interval $0 \leqslant \xi \leqslant 2\pi$. Differentiating Eq. (38) with respect to ξ, we obtain

$$d\phi = \frac{R\cos\xi + R^2}{1 + R^2 + 2R\cos\xi}\, d\xi \tag{40}$$

which, when substituted into Eq. (39), becomes

$$P(\phi,R)d\phi = \frac{1}{2\pi}\left[\left|\frac{1 + R^2 + 2R\cos\xi_1}{R\cos\xi_1 + R^2}\right| + \left|\frac{1 + R^2 + 2R\cos\xi_2}{R\cos\xi_2 + R^2}\right|\right] d\phi \ . \tag{41}$$

In order to have $P(\phi,R)$ as a function of ϕ and R only, it is necessary to find an expression for $R\cos\xi$. Employing a little trigonometric manipulation, Eq. (38) will yield

$$R\cos\xi = -\sin^2\phi \pm \cos\phi\sqrt{R^2 - \sin^2\phi} \ . \tag{42}$$

Combining Eqs. (41) and (42), there results after simplification

$$P(\phi,R)d\phi = \frac{1}{2\pi}\left[\left|1 + \frac{\cos\phi}{\sqrt{R^2 - \sin^2\phi}}\right| + \left|1 - \frac{\cos\phi}{\sqrt{R^2 - \sin^2\phi}}\right|\right] d\phi \ . \tag{43}$$

This is the required expression.

Equation (40) yields another useful result. If $d\theta/d\xi$ be equated to zero, there results

$$\cos\xi = -R \tag{44}$$

which, when substituted into Eq. (38), yields

$$\tan(\phi_{max}) = \frac{R}{\sqrt{1 - R^2}}$$

or

$$\sin(\phi_{max}) = R \quad . \tag{45}$$

That is, for any ratio of signal-to-noise greater than 1, ϕ has a maximum value given by Eq. (45). Conversely, for any ϕ, the minimum allowable R is given by Eq. (45). Therefore, the validity conditions on Eq. (43) may be stated in two ways, both of which must be satisfied simultaneously:

$$\begin{aligned} \sin\phi \leqslant R &\leqslant 1 \\ 0 \leqslant \phi &\leqslant \sin^{-1}R \quad . \end{aligned} \tag{46}$$

Case II

When $R > 1$, ϕ becomes a single-valued function of ξ. Therefore, the probability of ϕ lying in the interval $d\phi$ is the same as the probability of ξ being in $d\xi$:

$$P(\phi,R)d\phi = P(\xi)d\xi \quad . \tag{47}$$

This expression may be evaluated in a manner exactly analogous to that used in Case I. There results

$$P(\phi,R)d\phi = \frac{1}{2\pi}\left[1 + \frac{\cos\phi}{\sqrt{R^2 - \sin^2\phi}}\right]d\phi \quad . \tag{48}$$

The validity conditions on this expression are simply

$$\begin{aligned} 1 < R &< \infty \\ 0 \leqslant \phi &\leqslant 2\pi \quad . \end{aligned} \tag{49}$$

The probability densities, $P(\phi,R)$, for Cases I and II are shown in Fig. 15. These curves are plotted for positive values of ϕ only, since they are even functions of that variable. Note that the probability of ϕ falling in the interval $\Delta\phi$ is

$$\int_{\phi}^{\phi+\Delta\phi} P(\phi,R)d\phi \quad ,$$

an interval which proves to be finite regardless of the infinite portions of the densities for $R \leq 1$. In fact, it is easily shown that

$$\int_{0}^{\sin^{-1}R} P(\phi,R)d\phi = 1/2 \quad \text{for } R \leqslant 1$$

and

$$\int_0^{\pi} P(\phi,R)d\phi = 1/2 \quad \text{for } R > 1 \quad ,$$

a result which merely states that for any value of R, ϕ will certainly lie in the range given by Eq. (46) or Eq. (49).

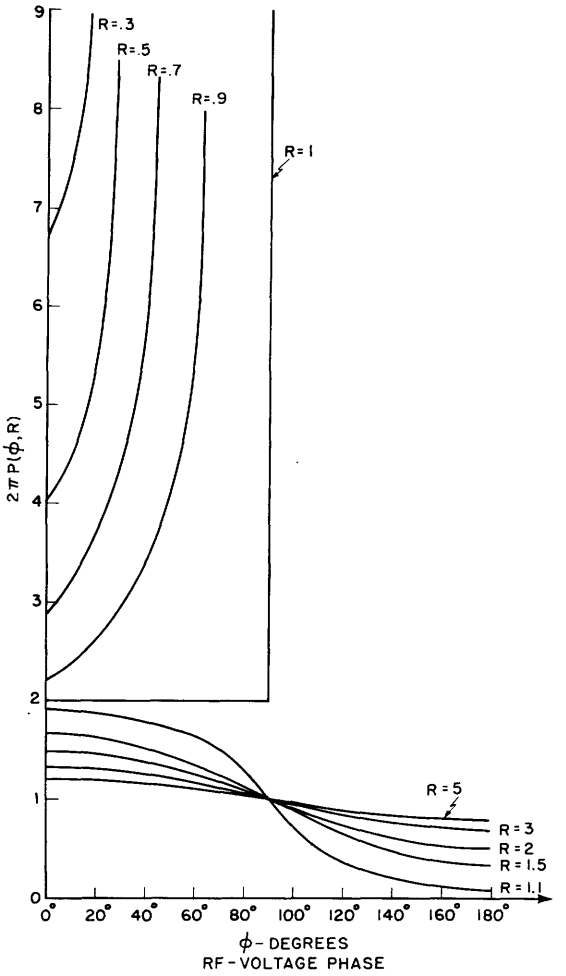

Fig. 15 Probability density of r-f voltage phase for constant values of noise amplitude.

It is now necessary to superpose the noise envelope distribution on our present solution. More specifically, this distribution may be written as a function of the variable R by consulting Eq. (36):

$$P(R)dR = 2R/\overline{R^2}\, e^{-R^2/\overline{R^2}}\, dR \quad , \tag{50}$$

where $\overline{R^2}$ is the noise-to-signal power ratio. Now it is easily seen that the probability of ϕ is merely the sum of all the $P(\phi,R)$ for all admissable R, multiplied by the weighting factor P(R). Therefore, in general,

$$P(\phi) = \int_0^{\infty} P(\phi,R)P(R)dR \quad . \tag{51}$$

In our case, this becomes

$$P(\phi) = 1/\pi\overline{R^2} \int_{\sin\phi}^{1} \left[\left| R\, e^{-R^2/\overline{R^2}} + \frac{R\cos\phi\, e^{-R^2/\overline{R^2}}}{\sqrt{R^2 - \sin^2\phi}} \right| + \left| R\, e^{-R^2/\overline{R^2}} - \frac{R\cos\phi\, e^{-R^2/\overline{R^2}}}{\sqrt{R^2 - \sin^2\phi}} \right| \right] dR$$

$$+ 1/\pi\overline{R^2} \int_{1}^{\infty} \left(R\, e^{-R^2/\overline{R^2}} + \frac{R\cos\phi\, e^{-R^2/\overline{R^2}}}{\sqrt{R^2 - \sin^2\phi}} \right) dR \qquad (52)$$

for $0 \leqslant \phi \leqslant \pi/2$. This expression may be evaluated by making the substitution $y^2 = R^2 - \sin^2\phi$, which results in

$$P(\phi) = 1/\pi\overline{R^2} \left\{ \left| \overline{R^2}/2 \left(e^{-\sin^2\phi/\overline{R^2}} - e^{-1/\overline{R^2}} \right) + \cos\phi\, e^{-\sin^2\phi/\overline{R^2}} \int_0^{\cos\phi} e^{-y^2/\overline{R^2}}\, dy \right| \right.$$

$$+ \left| \overline{R^2}/2 \left(e^{-\sin^2\phi/\overline{R^2}} - e^{-1/\overline{R^2}} \right) - \cos\phi\, e^{-\sin^2\phi/\overline{R^2}} \int_0^{\cos\phi} e^{-y^2/\overline{R^2}}\, dy \right| + \overline{R^2}/2\, e^{-1/\overline{R^2}}$$

$$\left. + \cos\phi\, e^{-\sin^2\phi/\overline{R^2}} \int_1^{\infty} e^{-y^2/\overline{R^2}}\, dy \right\} \qquad (53)$$

for $0 \leqslant \phi \leqslant \pi/2$. Now consider the integral

$$\int_0^{y_1} e^{-y^2/\overline{R^2}}\, dy \quad .$$

If we use the transformation $X = y/\sqrt{\overline{R^2}}$, we find

$$\int_0^{y_1} e^{-y^2/\overline{R^2}}\, dy = \sqrt{\overline{R^2}} \int_0^{x_1} e^{-x^2}\, dx \quad .$$

This then becomes

$$\sqrt{\overline{R^2}} \int_0^{x_1} e^{-x^2}\, dx = 2\sqrt{\frac{\overline{R^2}}{\pi}}\, \mathrm{erf}(x_1) \tag{54}$$

where $\mathrm{erf}(x_1)$ is the well-known error function. The expression for the probability density is then

$$\begin{aligned} P(\phi) = 1/\pi\overline{R^2} \Bigg\{ & \left| \overline{R^2}/2 \left(e^{-\sin^2\phi/\overline{R^2}} - e^{-1/\overline{R^2}} \right) \right. \\ & \left. + \sqrt{\pi\overline{R^2}/2}\, \cos\phi\, e^{-\sin^2\phi/\overline{R^2}}\, \mathrm{erf}(\cos\phi/\sqrt{\overline{R^2}}) \right| \\ & + \left| \overline{R^2}/2 \left(e^{-\sin^2\phi/\overline{R^2}} - e^{-1/\overline{R^2}} \right) \right. \\ & \left. - \sqrt{\pi\overline{R^2}/2}\, \cos\phi\, e^{-\sin^2\phi/\overline{R^2}}\, \mathrm{erf}(\cos\phi/\sqrt{\overline{R^2}}) \right| + \overline{R^2}/2\, e^{-1/\overline{R^2}} \\ & + \sqrt{\pi\overline{R^2}/2}\, \cos\phi\, e^{-\sin^2\phi/\overline{R^2}} \left[1 - \mathrm{erf}(1/\sqrt{\overline{R^2}}) \right] \Bigg\} \end{aligned} \tag{55}$$

for $0 \leqslant \phi \leqslant \pi/2$ where the limitation on ϕ may be deduced from Eq. (46). For $\pi/2 \leqslant \phi \leqslant \pi$, we have

$$\begin{aligned} P(\phi) &= 1/\pi\overline{R^2} \int_1^{\infty} \left(R e^{-R^2/\overline{R^2}} + \frac{R\cos\phi\, e^{-R^2/\overline{R^2}}}{\sqrt{R^2 - \sin^2\phi}} \right) dR \\ &= 1/\pi\overline{R^2} \left\{ R^2/2\, e^{-1/\overline{R^2}} + \sqrt{\pi\overline{R^2}/2}\, \cos\phi\, e^{-\sin^2\phi/\overline{R^2}} \left[1 - \mathrm{erf}\, 1/\sqrt{\overline{R^2}} \right] \right\} . \end{aligned} \tag{56}$$

Figure 16 shows these probability densities plotted from Eqs. (55) and (56) for various values of noise-to-signal ratio. Fig. 17 shows

$$P(0,\phi) = \int_0^{\phi} P(\phi)\, d\phi \quad ,$$

the probability of the initial phase falling in interval $0 - \phi$. These curves were obtained from those of Fig. 16 by graphical integration and are, of course, also even functions of ϕ. We have established, therefore, the probability of initial phase as a function of noise-to-signal ratio. With this information available, we may now proceed to set up and solve the differential equation for magnetron starting in the presence of an externally applied sinusoidal signal.

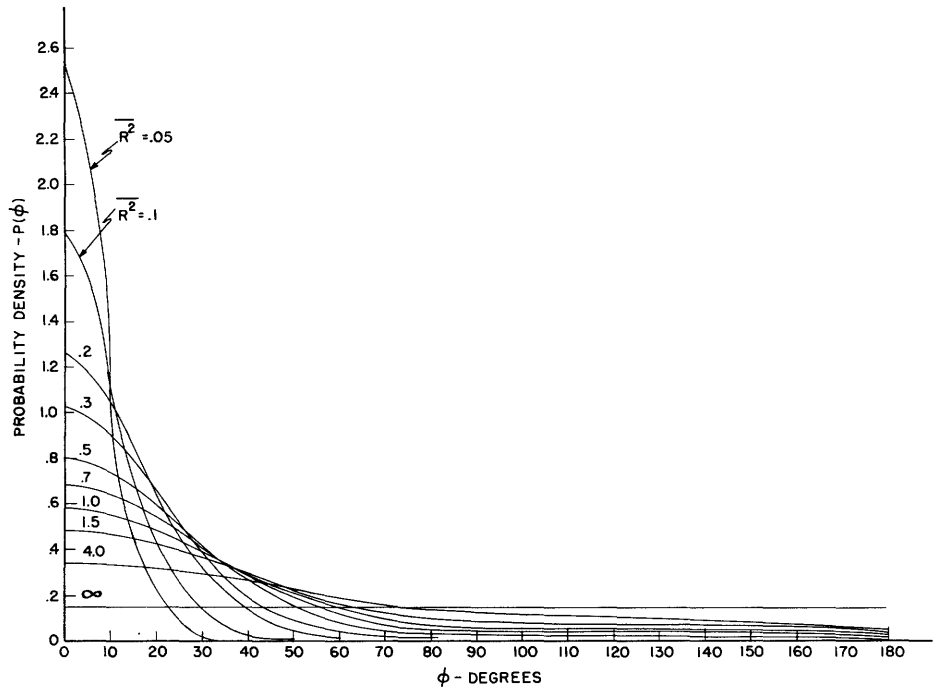

Fig. 16 Probability density of phase of sine wave plus noise with noise-to-signal ratio as a parameter.

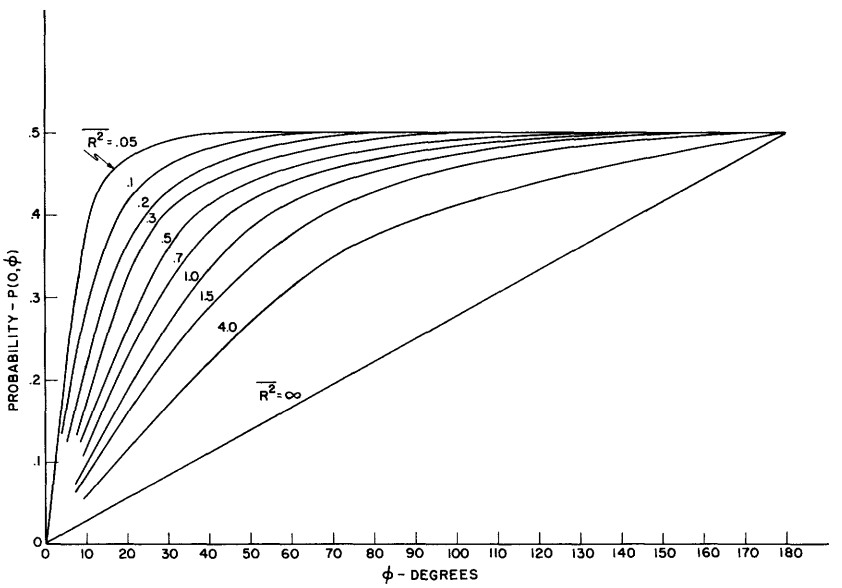

Fig. 17 The probability $P(0,\phi) = \int_0^{\phi} P(\phi)d\phi$ with noise-to-signal ratio as a parameter.

VII. The Starting Equation

It has been found experimentally ((2) pp. 489-95), (4) that the electronic behavior of the steady-state magnetron may be described approximately by the two relations

$$g = \frac{E/R}{V_{RF}} - \frac{1}{R} \tag{57}$$

$$b = \beta - g \tan\alpha \tag{58}$$

where E, R, β, and α are constants which change with d-c conditions. If the starting of a magnetron is considered as a quasi-steady-state process, that is, a succession of steady-states, then Eqs. (57) and (58), together with the oscillator operating equations, may be used to write a differential equation of starting. Such an analysis has been carried out by Slater (2), Rieke (5), and others (see bibliography) with the result that the r-f envelope during starting may be represented* as

$$v_{rf} = V_{RF_o}(1 - e^{-kt}) \tag{59}$$

where V_{RF_o}, the steady-state value of v_{rf}, and k, the reciprocal of the build-up time constant, are evaluated as functions of the design and steady-state properties of the magnetron. It has been found experimentally that at small r-f voltage Eq. (59) is not a good approximation of true conditions. During the beginning of the build-up, the r-f voltage increases exponentially, a condition impossible unless g is constant. Equation (57), therefore, is valid only after the initial instant of starting. If a locking signal is present, however, quite a large r-f voltage may already exist at this first instant. Under these conditions, it is probable that the build-up follows Eq. (59) closely even at the beginning. Of course, if the locking signal is quite small, the exponential behavior will doubtlessly be present. In either case, it is desirable to rewrite Eq. (59) as

$$v_{rf} = V_{RF_o}(1 - \eta e^{-kt}) \tag{60}$$

where η is a constant whose value lies between 0.7 and 1. Equation (60) states that at t = 0, the time at which the build-up has progressed far enough for Eq. (57) to be valid, the r-f anode voltage is finite and has the value

$$v_{rf_i} = (1 - \eta)\, V_{RF_o} \quad . \tag{61}$$

---

* See Appendix II for derivation.

Subsequent to this time, the build-up continues exactly as expressed by Eq. (59). Actual observations on magnetron r-f build-up show η to be 0.8, or greater in most cases. The experimental evidences show the above theory to be a good approximation so long as the r-f load is not badly mismatched.*

Equation (60) expresses the form of the r-f build-up envelope; however, nothing has been said about the frequency and phase during the transient period. This information is readily obtained by use of Eqs. (57) and (58):

$$g = \frac{E/R}{V_{RF}} - \frac{1}{R} = \frac{E/R}{V_{RF_o}(1 - \eta e^{-kt})} - \frac{1}{R}$$

or

$$g = \frac{E/R}{V_{RF_o}} - \frac{1}{R} + \frac{E/R}{V_{RF_o}} \frac{\eta e^{-kt}}{(1 - e^{-kt})}$$

or

$$g = g_o + \frac{E\eta}{RV_{RF_o}} \frac{e^{-kt}}{1 - \eta e^{-kt}} \tag{62}$$

where g_o is the steady-state electronic conductance. Then from Eq. (58),

$$b = \beta - g_o \tan\alpha - \frac{E\eta}{RV_{RF_o}} \left(\frac{e^{-kt}}{1 - \eta e^{-kt}}\right) \tan\alpha$$

$$b = b_o - \frac{E\eta}{RV_{RF_o}} \tan\alpha \left(\frac{e^{-kt}}{1 - \eta e^{-kt}}\right) \tag{63}$$

where b_o is the steady-state electronic susceptance. Using the same magnetron operating equation as before,

$$\frac{b}{\omega_o C} = 2\left(\frac{\omega - \omega_o}{\omega_o}\right) + \frac{B}{Q_{ext}} = \frac{b_o}{\omega_o C} - \frac{E\eta}{\omega_o C V_{RF_o} R} \tan\alpha \left(\frac{e^{-kt}}{1 - \eta e^{-kt}}\right) \tag{64}$$

or

$$2\left(\frac{\omega - \omega'}{\omega_o}\right) = - \frac{E\eta}{\omega_o C R V_{RF_o}} \tan\alpha \left(\frac{e^{-kt}}{1 - \eta e^{-kt}}\right) \tag{65}$$

where $\omega' = 2b_o/C - \omega_o B/2Q_{ext} + \omega_o$ = steady-state operating frequency.

Further simplification yields

$$\omega = \omega' - \left(\frac{E\eta}{2CRV_{RF_o}} \tan\alpha\right)\left(\frac{e^{-kt}}{1 - \eta e^{-kt}}\right) . \tag{66}$$

This result shows that the frequency of the magnetron during the initial

* W. Rotman, a study of transient phenomena in magnetrons, unpublished notes, R.L.E., M.I.T., March 18, 1948.

part of the build-up may be remote from the steady-state value ω'. Rotman's measurements on steady-state and transient g - V_{RF} relations, when used to evaluate Eq. (66) for t = 0, indicate that the frequency difference may be as much as 20 Mc. Further experimental evidence is necessary, however, before an absolute evaluation is made.

With this understanding of magnetron starting, we may now derive an equation expressing the phase of the magnetron during build-up when an external, sinusoidal signal is impressed. The synchronizing signal is considered small enough so that the fundamental nature of the build-up is not disturbed. It is shown in Appendix I that the load susceptance of a synchronized oscillator is approximately

$$B' = B - 2|\rho| \sin\Phi$$

where B is the passive susceptance, Φ is the locking phase, and

$$|\rho| = \left|Y_{LP}\rho_s\right| = \left|Y_{LP}\right| \left|\frac{V_1}{V_i}\right|$$

where Y_{LP} is the passive load admittance, and V_1/V_i is the ratio of locking voltage to magnetron incident voltage at the magnetron reference plane. During starting, then, the reflection factor becomes

$$|\rho| = \left|Y_{LP}\right| \left|\frac{V_1}{V_{RF_o}(1 - \eta e^{-kt})}\right| = \left|Y_{LP}\right| \left|\frac{V_1}{V_{RF_o}}\right| \left(\frac{1}{1 - \eta e^{-kt}}\right). \quad (67)$$

This expression is a good approximation so long as V_1/V_{RF_o} is considerably less than the quantity $(1 - \eta)$. Now V_1 is the total voltage at the reference plane due to the locking signal. This voltage includes that caused by the wave incident on the magnetron cavity and that reflected from it. During the build-up, therefore, V_1 may also be a function of time. The nature of the variation depends on the locking frequency, the steady-state oscillator load, and the variation of electronic admittance with time. An exact evaluation of this effect is difficult and, for our purposes, unnecessary, since we are interested in qualitative rather than quantitative results at the moment. It is easy to see, however, how changes in V_1 will effect $|\rho|$ as a function of time. If V_1 is considered constant, Eq. (67) shows that $|\rho|$ is large at t = 0 and decreases exponentially to its steady-state value as t increases. Actually, V_1 starts at some small value and increases with time, so that the variation shown by Eq. (67) is exaggerated in magnitude. That is, the initial value of $|\rho|$ is not so large as indicated, but, nevertheless, may exceed the steady-state $|\rho|$ considerably. An assumption of constant V_1, therefore, will not change the fundamental nature of the solu-

tion, although it will exaggerate the effect of the locking signal. In our solution, Eq. (67) will be used to represent the reflection factor as a function of time. We should expect, then, that synchronization will be indicated earlier in time than is actually the case. In this respect, the solution will be an optimistic one.

With this approximation in mind, we may write down the differential equation of starting. Again using Eq. (64), and substituting the expression for B', we have

$$\frac{b_o}{\omega_o C} - \frac{E\eta}{\omega_o CRV_{RF_o}} \tan\alpha \left(\frac{e^{-kt}}{1 - \eta e^{-kt}}\right) = 2\left(\frac{\omega - \omega_o}{\omega_o}\right) + \frac{B}{Q_{ext}} - \frac{2|\rho_o|}{Q_{ext}} \left(\frac{\sin\phi}{1 - \eta e^{-kt}}\right)$$

$$\text{or} \qquad 2\left(\frac{\omega - \omega'}{\omega_o}\right) + \frac{E\eta}{\omega_o CRV_{RF_o}} \left(\frac{e^{-kt}}{1 - \eta e^{-kt}}\right) - 2\frac{|\rho_o|}{Q_{ext}} \left(\frac{\sin\phi}{1 - \eta e^{-kt}}\right) = 0 \qquad (68)$$

where $\omega' = 2b_o/C - \omega_o B/2Q_{ext} + \omega_o$, the steady-state operating frequency with no impressed locking signal, and $|\rho_o|$ is the steady-state reflection factor. Now if ω_1 is the frequency of the synchronizing signal,

$$\frac{d\phi}{dt} = \omega_1 - \omega \quad . \qquad (69)$$

If this be substituted into Eq. (68), there results

$$\frac{d\phi}{dt} + \left(\frac{S}{1 - \eta e^{-kt}}\right) \sin\phi = M + \frac{Ne^{-kt}}{1 - \eta e^{-kt}} \qquad (70)$$

where $S = \omega_o|\rho_o|/Q_{ext}$, $M = \omega_1 - \omega'$, and $N = E\eta/2CRV_{RF_o} \tan\alpha$. This is the differential equation of starting which was desired. We need only solve the equation in order to find the phase ϕ as a function of time with the steady-state properties of the system as parameters.

The steady-state portion of the solution is the same as that discussed in Appendix I, for if t be allowed to approach infinity, Eq. (70) becomes indentical with Eq. (I-10). The analytical solution of this equation has been discussed by Slater, Adler, and others. Briefly, if $M/S \leqslant 1$, a stable lock-in occurs ($d\phi/dt = 0$); while if $M/S > 1$, synchronization is not accomplished and ϕ becomes a continuously increasing function.

Unfortunately, Eq. (70) is non-linear in the dependent variable ϕ, so that an explicit analytical solution is not to be expected. The nature of the solution may be deduced by considering the equation for small values of ϕ only, so that $\sin\phi$ may be replaced by ϕ. Such a study is made in the following section. If more information is desired, machine methods are available which give a complete solution for particular values of the coefficients. Results of this type are discussed in the final section.

VIII. An Approximate Solution

An analytical expression for the phase as a function of time may be obtained from Eq. (70), provided we are interested in the solution for small ϕ only. If this is the case, $\sin\phi$ may be replaced by ϕ, and Eq. (70) becomes an ordinary linear differential equation:

$$\frac{d\phi}{dt} + \left(\frac{S}{1 - \eta e^{-kt}}\right)\phi = M + \frac{Ne^{-kt}}{1 - \eta e^{-kt}} \quad . \tag{71}$$

It may be solved by use of an integrating factor $e^{\int P dt}$ where P is the coefficient of the term in ϕ. In this case

$$\int P dt = \frac{S}{k}\left[kt + \ln(1 - \eta e^{-kt})\right]$$

$$= St + \ln(1 - \eta e^{-kt})^{S/k}$$

or $$e^{\int P dt} = e^{St}(1 - \eta e^{-kt})^{S/k} \quad .$$

If Eq. (71) be multiplied by this factor and integrated, there results

$$e^{St}(1 - \eta e^{-kt})^{S/k}\phi =$$

$$\int\left[Me^{St}(1 - \eta e^{-kt})^{S/k} + Ne^{(S-k)t}(1 - \eta e^{-kt})^{S/k-1}\right] dt \quad . \tag{72}$$

The indicated integrations are not difficult to carry out if the factors

$$(1 - \eta e^{-kt})^{S/k}$$

and $$(1 - \eta e^{-kt})^{S/k-1}$$

are expanded in series by the binomial expansion. In particular,

$$(1 - \eta e^{-kt})^{x} = 1 - x\eta e^{-kt} + \frac{x(x-1)}{2!}\eta^2 e^{-2kt} - \frac{x(x-1)(x-2)}{3!}\eta^3 e^{-3kt}$$

$$+ \ldots (-1)^n \frac{x!\eta^n e^{-nkt}}{(x-n)!n!} + \ldots \quad .$$

Therefore,

$$\int e^{St}(1 - \eta e^{-kt})^{\frac{S}{k}} dt = \frac{e^{St}}{S} - \frac{\frac{S}{k}}{S - k}\eta e^{-(S-k)t} + \frac{\frac{S}{k}\left(\frac{S}{k} - 1\right)}{2!(S - 2k)}\eta^2 e^{(S-2k)t}$$

$$- \frac{\frac{S}{k}(\frac{S}{k} - 1)(\frac{S}{k} - 2)}{3!(S - 2k)} \eta^3 e^{(S-3k)t} \cdots$$

$$= \frac{e^{St}}{S} + \sum_{m=1}^{\infty} (-1)^m \frac{\frac{S}{k}(\frac{S}{k} - 1)\cdots(\frac{S}{k} + 1 - m)}{k\, m!(\frac{S}{k} - m)} \eta^m e^{(S-mk)t}$$

and, similarly,

$$\int e^{(S-k)t} (1 - \eta e^{-kt})^{\frac{S}{k}-1} dt$$

$$= \frac{e^{(S-k)t}}{S - 1k} + \sum_{m=1}^{\infty} (-1)^m \frac{(\frac{S}{k} - 1)(\frac{S}{k} - 2)\cdots(\frac{S}{k} - m)}{k\, m!(\frac{S}{k} - m - 1)} \eta^m e^{(S-m-1)t} .$$

Then Φ may be written

$$\Phi = \frac{1}{(1 - \eta e^{-kt})^{\frac{S}{k}}} \left[\frac{M}{S} + M \sum_{m=1}^{\infty} (-1)^m \frac{\frac{S}{k}(\frac{S}{k} - 1)\cdots(\frac{S}{k} + 1 - m)}{k\, m!(\frac{S}{k} - m)} \eta^m e^{-mkt} \right.$$

$$\left. + \frac{N}{k(\frac{S}{k} - 1)} e^{-kt} + N \sum_{m=1}^{\infty} (-1)^m \frac{(\frac{S}{k} - 1)(\frac{S}{k} - 2)\cdots(\frac{S}{k} - m)}{k\, m!(\frac{S}{k} - m - 1)} \eta^m e^{-(m+1)t} + \Phi' e^{-St} \right] \tag{73}$$

where Φ' is a constant of integration. If the factor

$$(1 - \eta e^{-kt})^{\frac{S}{k}}$$

be expanded in a series and divided into the bracketed series, there results

$$\Phi = \frac{1}{(1 - \eta e^{-kt})^{\frac{S}{k}}} \left[\frac{M}{S} + \frac{N - \eta M}{k(\frac{S}{k} - 1)} e^{-kt} + \Phi' e^{-St} \right]$$

$$+ \frac{N - \eta M}{\eta} \sum_{m=1}^{\infty} (-1)^m \frac{m!\eta^{m+1} e^{-(m+1)kt}}{k(\frac{S}{k} - 1)(\frac{S}{k} - 2)\cdots(\frac{S}{k} - m - 1)} . \tag{74}$$

The constant Φ' may be evaluated by utilizing the initial conditions which have been discussed previously. Specifically, when $t = 0$, $\Phi = \Phi_o$, an angle determined statistically by the vector sum of preoscillation noise and locking signal. Then

$$\Phi_o = \frac{1}{(1 - \eta)^{\frac{S}{k}}} \left[\frac{M}{S} + \frac{N - \eta M}{k(\frac{S}{k} - 1)} + \Phi' \right]$$

$$+ \frac{N - \eta M}{\eta} \sum_{m=1}^{\infty} (-1)^m \frac{m! \eta^{m+1}}{k(\frac{S}{k} - 1)(\frac{S}{k} - 2)\ldots(\frac{S}{k} - m - 1)} \quad . \tag{75}$$

Equation (75) may be solved for ϕ', and then the solution for ϕ becomes

$$\phi = \frac{1}{(1 - \eta e^{-kt})^{\frac{S}{k}}} \left\{ \frac{M}{S} + \frac{N - \eta M}{k(\frac{S}{k} - 1)} e^{-kt} + \left[(1 - \eta)^{\frac{S}{k}} \phi_o - \frac{M}{S} - \frac{N - \eta M}{k(\frac{S}{k} - 1)} \right. \right.$$

$$\left. \left. - (1 - \eta)^{\frac{S}{k}} (\frac{N - \eta M}{\eta}) \sum_{m=1}^{\infty} (-1)^m \frac{m! \eta^{m+1}}{k(\frac{S}{k} - 1)\ldots(\frac{S}{k} - m - 1)} \right] e^{-St} \right\}$$

$$+ \frac{N - \eta M}{\eta} \sum_{m=1}^{\infty} (-1)^m \frac{m! \eta^{m+1} e^{-(m+1)kt}}{k(\frac{S}{k} - 1)(\frac{S}{k} - 2)\ldots(\frac{S}{k} - m - 1)} \quad . \tag{76}$$

Interpretation of this result is facilitated if the constants involved are evaluated within an order of magnitude. Although sparse experimental evidence is available for this purpose, some information may be obtained from data published by the M.I.T. Radiation Laboratory (5). The majority of these data describe the operation of a 3,000-Mc magnetron. Therefore, the numbers deduced therefrom are believed representative of this type oscillator operating in the 10-cm region.

The constant S is defined as $S = \omega_o |\rho_o| / Q_{ext}$. Its value ranges approximately from 10^6 to 5×10^7 for typical S-band magnetrons. Note that it is directly proportional to the square-root of the synchronizing power and inversely related to the product of external Q and square-root of power output. We may say, therefore, that its value indicates in a quantitative manner the effect of the locking signal.

The time-constant of the r-f voltage build-up is 1/k. Direct observations by means of high-speed oscillographs indicate that a value of about 10^{-8} sec is typical. This constant is a function of the oscillator resonant frequency, loaded Q, and electronic characteristics.* Now k and N may be related by means of the expressions derived in Appendix II. There it is shown that

$$N = k\eta \tan\alpha = \eta \times 10^{-8} \tan\alpha \quad . \tag{77}$$

The value of $\tan\alpha$ ranges approximately between the limits 0.1 and 1, and, as previously stated, η lies between 0.7 and 1.

Thus it is seen that the constants k, N, and η are intimately related to the electronics of the oscillator, while S and M reflect the character

* See Appendix II.

of the locking signal. The latter, therefore, are the primary operating parameters of the system, while the former are related to the design. Of course, this separation is not absolute, since all are functions of design and operating conditions, but it does indicate in a qualitative manner the most important factors determining the constants. With these concepts in mind, we may now examine our approximate solution.

In almost all practical cases of synchronization, the frequencies ω_1 and ω' are made as nearly equal as possible, and the phenomenon is used merely as a "phasing" device. Let us first consider $M = \omega_1 - \omega' = 0$ and also assume that the preoscillation noise is small, so that the initial angle, ϕ_o, is zero. The final phase, of course, will also be zero, since $\phi_{ss} = M/S = 0$. Fig. 18 shows the form of the phase transient under these conditions for various values of S. Note that the phase is disturbed quite

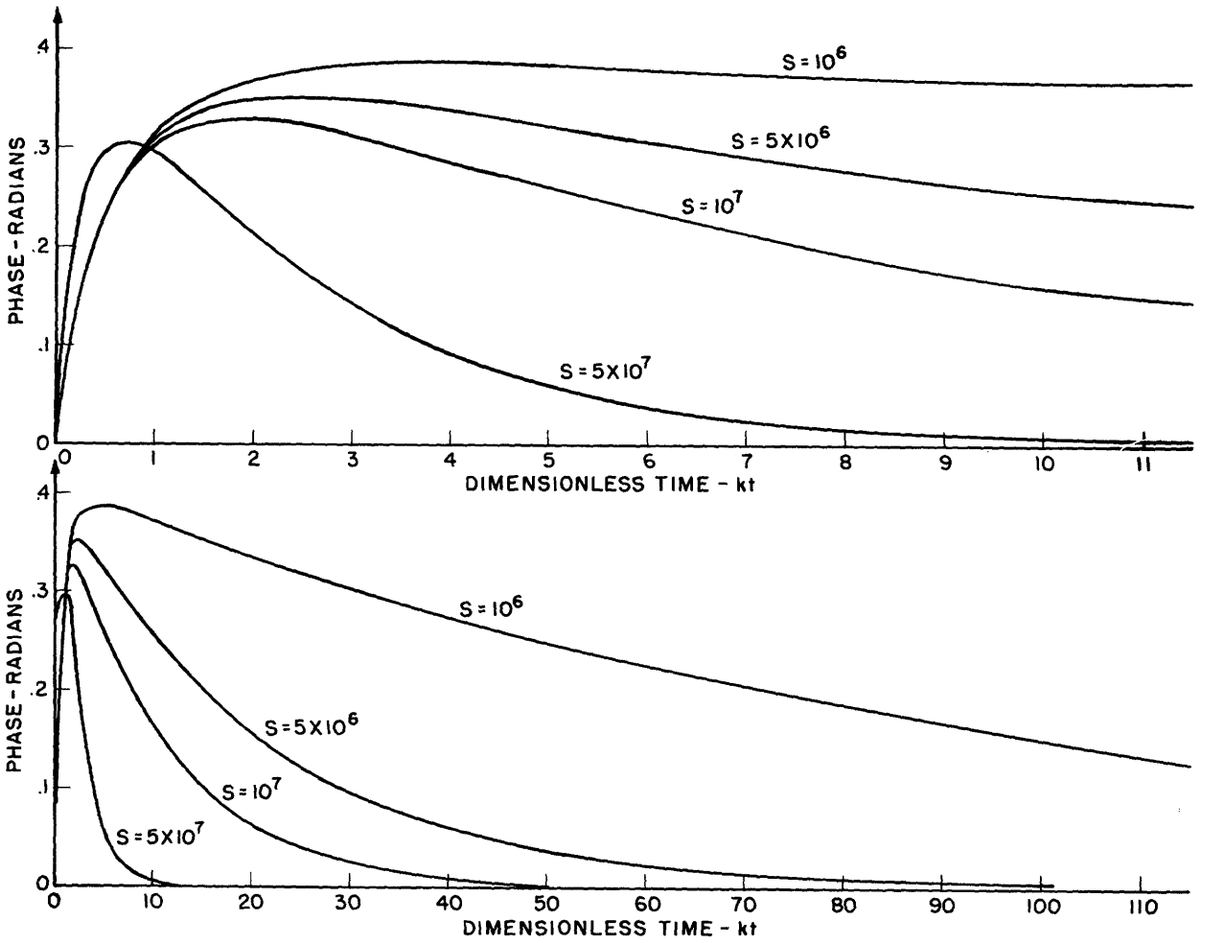

Fig. 18 Phase transient accompanying the starting of a synchronized magnetron with locking power as a parameter for $M = 0$, $N = 2 \times 10^7$, $k = 10^8$, $\phi_o = 0$, and $\eta = 0.8$.

violently during the magnetron voltage build-up. This effect results from frequency modulation of the tube during the starting period as described earlier for the unsynchronized case. It is interesting to note that this electronic frequency pushing is present regardless of the locking signal. Remembering that the magnetron commences its build-up in an essentially linear fashion (g, b constant), this behavior is not unexpected, for a linear oscillator is not susceptible to synchronization. Only self-limiting (non-linear) systems exhibit this phenomenon. After this initial perturbation, the phase approaches its steady-state value exponentially with a time constant 1/S. The values of η and N^* do not greatly affect the form of the transient; however, the magnitude of the disturbance increases quite rapidly with both, as can be seen by noting that the initial frequency difference is $d\phi/dt|_{t=0}$ and

$$\frac{d\phi}{dt}\Big|_{t=0} = \omega_1 - \omega|_{t=0} = \frac{N}{1-\eta} \tag{78}$$

The instantaneous frequency difference, $d\phi/dt$, is shown in Fig. 19 for the same values of S as in Fig. 18. Here the frequency modulation effect is quite apparent.

Preoscillation noise present in the magnetron will cause the initial angle, ϕ_o, to be different from zero. How this condition affects the phase transient is shown in Fig. 20. Note that since the duration of the transient is much greater than that of the magnetron voltage build-up, the consequences of the preoscillation noise are evident for a comparatively long period. Hence, the state of the oscillator at the first instant of starting is of paramount importance if a high degree of phase coherence from pulse-to-pulse is desired. Another consideration of equal importance is, of course, that of variations in the d-c pulse voltage, as discussed in the first sections of this report. The effect of such variations is to make M, and therefore the steady-state phase M/S, different from zero. Figures 21 and 22 show the phase transient for M/S = 0.348 and -0.348 respectively. The actual magnitude of the steady-state incoherence (M/S) resulting from a particular voltage change may be computed exactly as has been described in Section III.

It may be seen quite clearly from Figs. 21 and 22 that the operation of a pulsed synchronized magnetron is different for positive and negative values of the frequency difference, $\omega_1 - \omega'$. This characteristic has been noted very distinctly in experimental circuits.

We have now examined the solution of Eq. (70) for small ϕ. A more general solution, obtained by machine methods, will be presented in Section IX.

* The values $N = 2 \times 10^7$ and $\eta = 0.8$ were computed from data on a QK-61 magnetron. The corresponding value for S is 5×10^6 if $|\rho| = 0.1$.

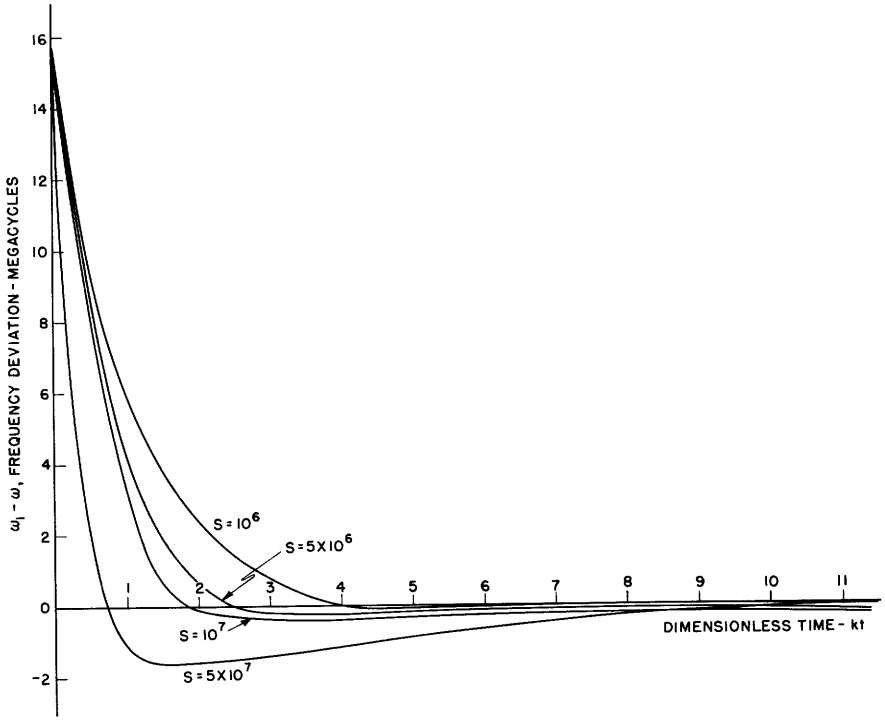

Fig. 19 Frequency transient accompanying the starting of a synchronized magnetron for: $M = 0$, $N = 2 \times 10^7$, $k = 10^8$, $\phi_o = 0$, $\eta = 0.8$.

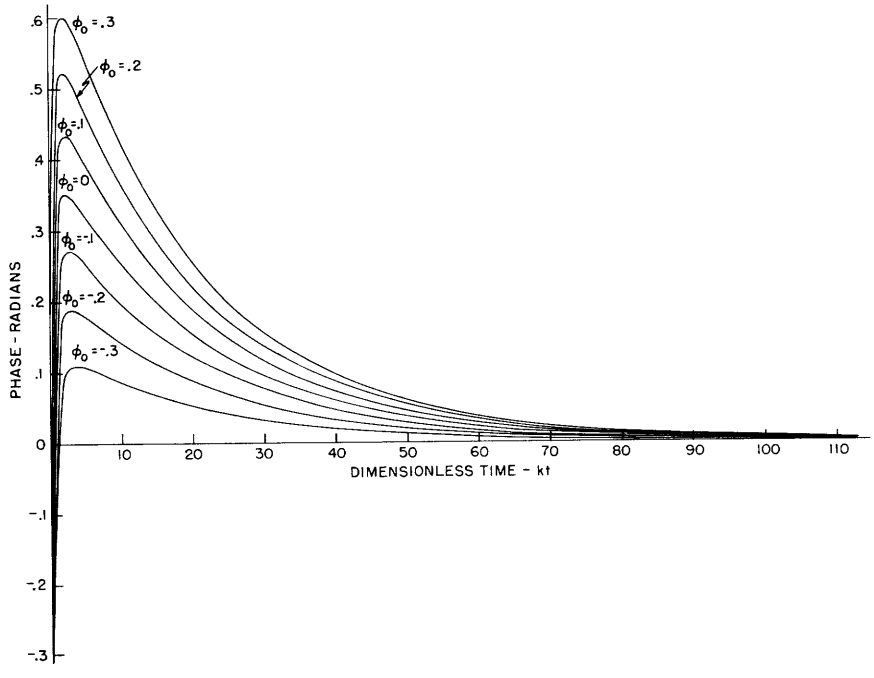

Fig. 20 Effect of initial conditions on phase transient for: $M = 0$, $N = 2 \times 10^7$, $k = 10^8$, $\eta = 0.8$, $S = 5 \times 10^6$.

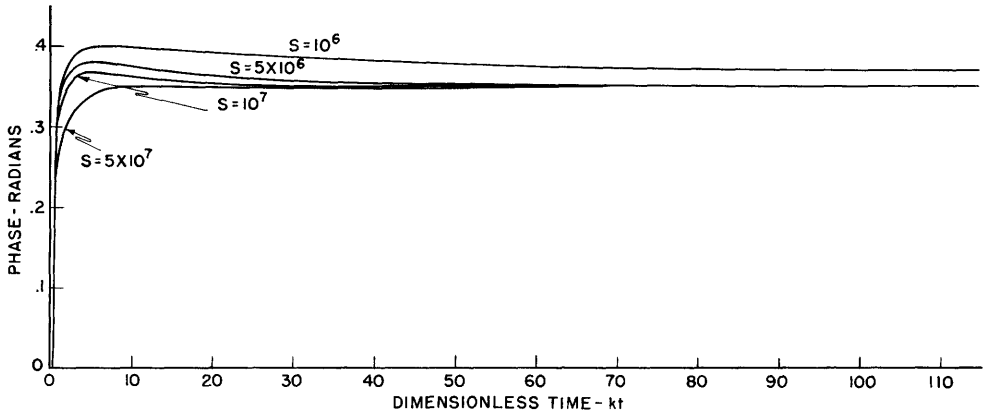

Fig. 21 Phase transient accompanying the starting of a synchronized magnetron with locking power as a parameter for $M/S = 0.348$, $N = 2 \times 10^7$, $k = 10^8$, $\phi_o = 0$, $\eta = 0.8$.

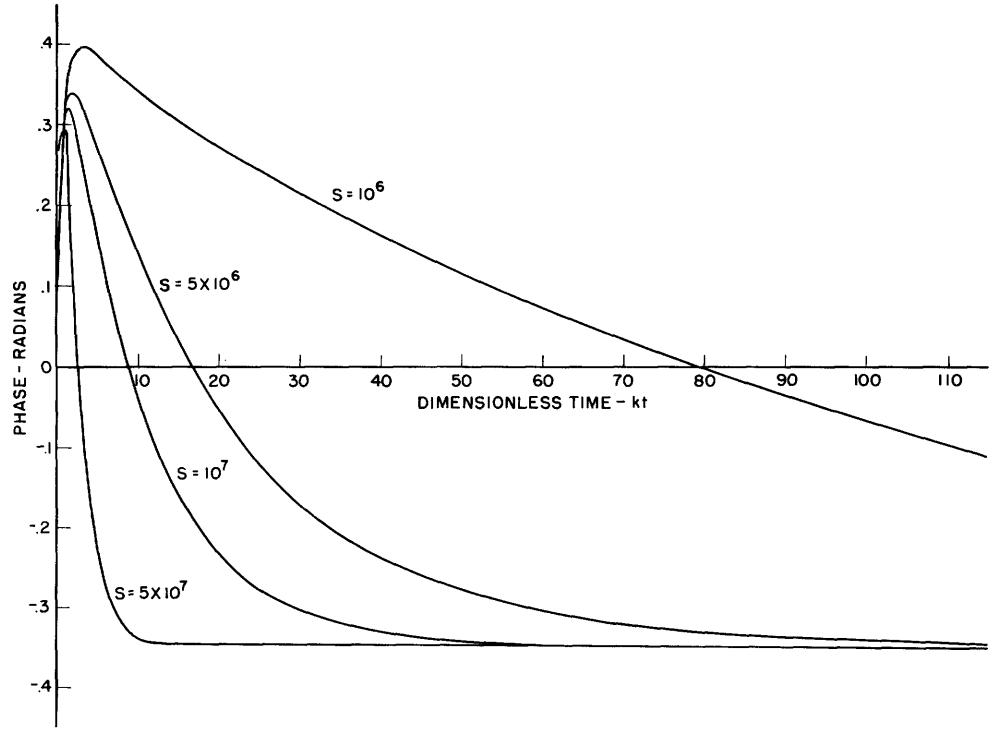

Fig. 22 Phase transient accompanying the starting of a synchronized oscillator with locking power as a parameter for $M/S = -0.348$, $N = 2 \times 10^7$, $k = 10^8$, $\phi_o = 0$, $\eta = 0.8$.

IX. Solution of the Starting Equation for Large Values of Φ

The use of analogue computers is the most powerful method presently available for obtaining the solution to non-linear differential equations. Such a computer has been designed and constructed by Dr. A. B. Macnee of the Research Laboratory of Electronics at M.I.T. (6). It is through the use of this machine, and with Dr. Macnee's assistance, that the solutions presented in this section were obtained.

Sources of error in these solutions are two-fold. First, calibration errors may be as much as 10 percent. Second, an important part of the transient occurs within a time comparable with the time-constant of the analyzer itself. The initial portion of these solutions, therefore, is considerably in error.

Figure 23a shows the phase Φ as a function of time for values of S when the frequency difference, $M = \omega_1 - \omega'$, is 5 megaradians per second. Note that when the quantity M/S becomes greater than one, there is no longer sufficient synchronizing power to maintain locking and the phase becomes a continuously increasing function. The frequency for this condition, along with that for the locked case, is shown in Fig. 23b. The periodic variations of frequency are typical of the unsynchronized oscillator when perturbed by an external signal. Figures 24a and 24b show phase and frequency for the same conditions except that $M = \omega_1 - \omega'$ is negative.

How variations in $|\omega_1 - \omega'|$ affect the phase and frequency with S constant is shown in Figs. 25a and 25b. The similarity to Figs. 23 and 24 should be noted.

The effect of initial angles -60°, 0°, and 60° when M/S is 0.95 is depicted in Figs. 26a and 26b. It is seen that a large positive or negative initial angle considerably increases the magnitude and duration of the transient. This effect is shown more graphically in Figs. 27 and 28 where $\Phi_o = \pm 180°$. Under such conditions, the transient becomes quite intense and synchronization does not occur until almost a microsecond has elapsed. Since in some applications the pulse length is considerably shorter than the duration of the transient, it is again seen that preoscillation noise can give rise to large incoherencies. Of course, the probability of such conditions may be reduced to insignificance by the use of large synchronizing power.

Thus the exact solution to the starting equation shows the same general character as does the approximate solution introduced in Section VIII. Both solutions emphasize the importance of the preoscillation state when pulse-to-pulse coherence is desired. Finally, the preoscillation noise-to-locking signal ratio is the important parameter determining this condition.

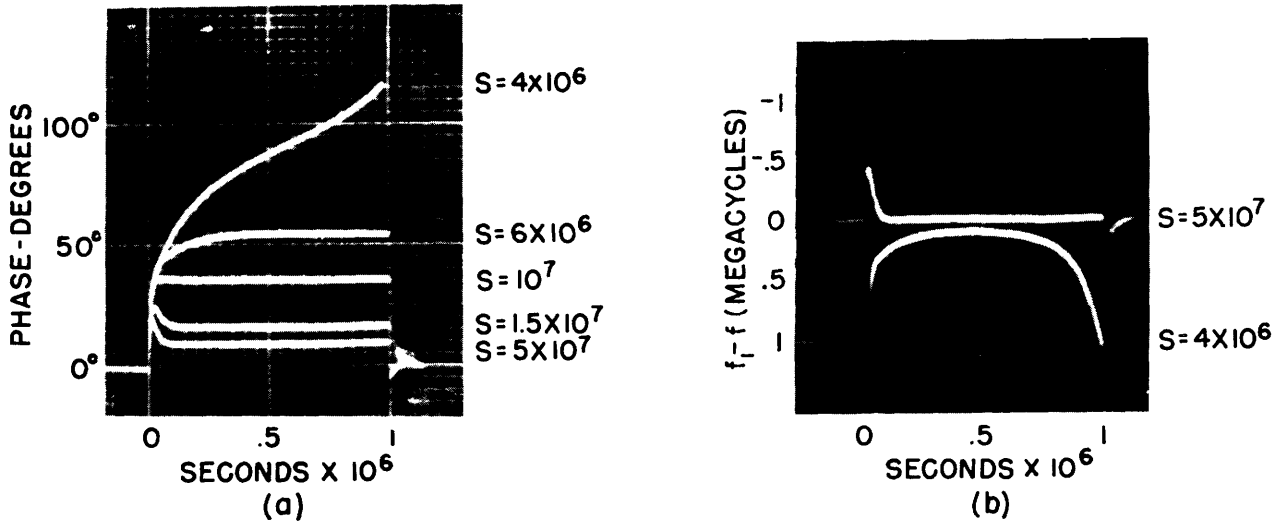

Fig. 23 Phase and frequency for M = 5 megaradians showing the effect of changes in synchronizing power.

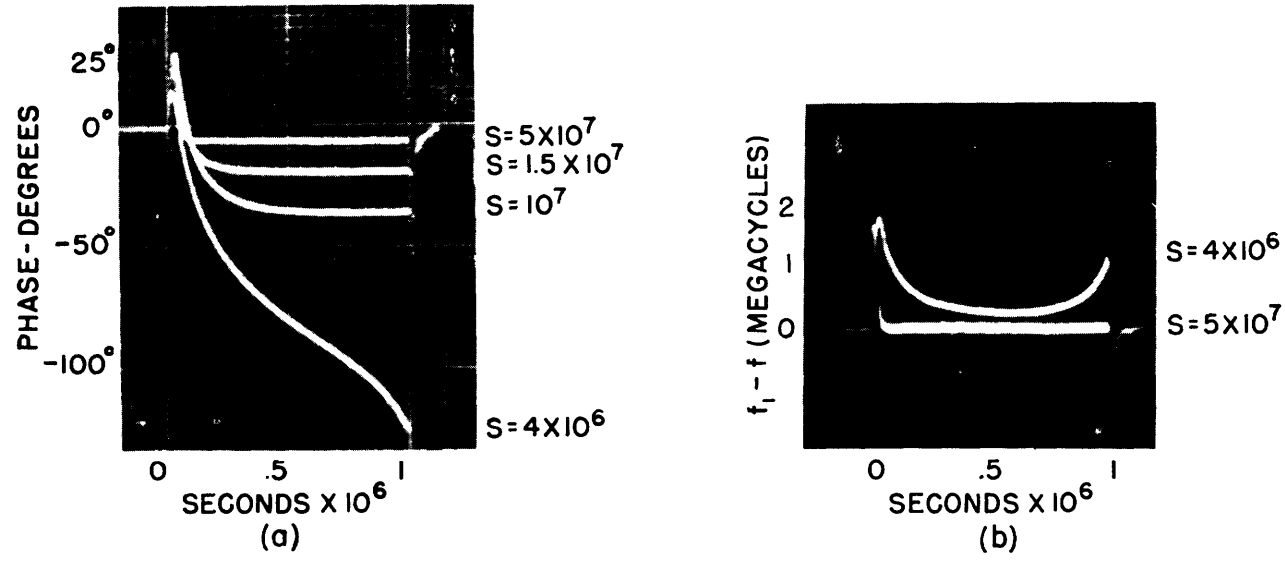

Fig. 24 Phase and frequency for M = -5 megaradians showing the effect of changes in synchronizing power.

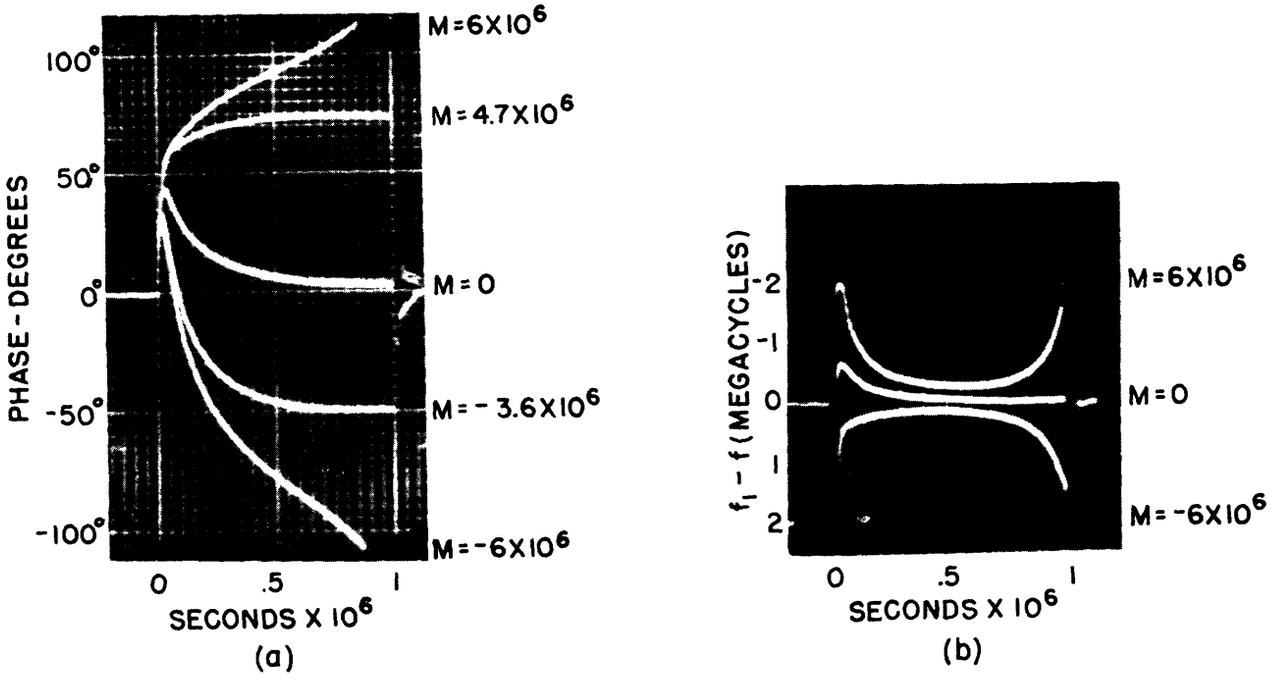

Fig. 25 Phase and frequency for $S = 5 \times 10^6$ showing effect of changes in frequency difference $\omega_1 - \omega'$.

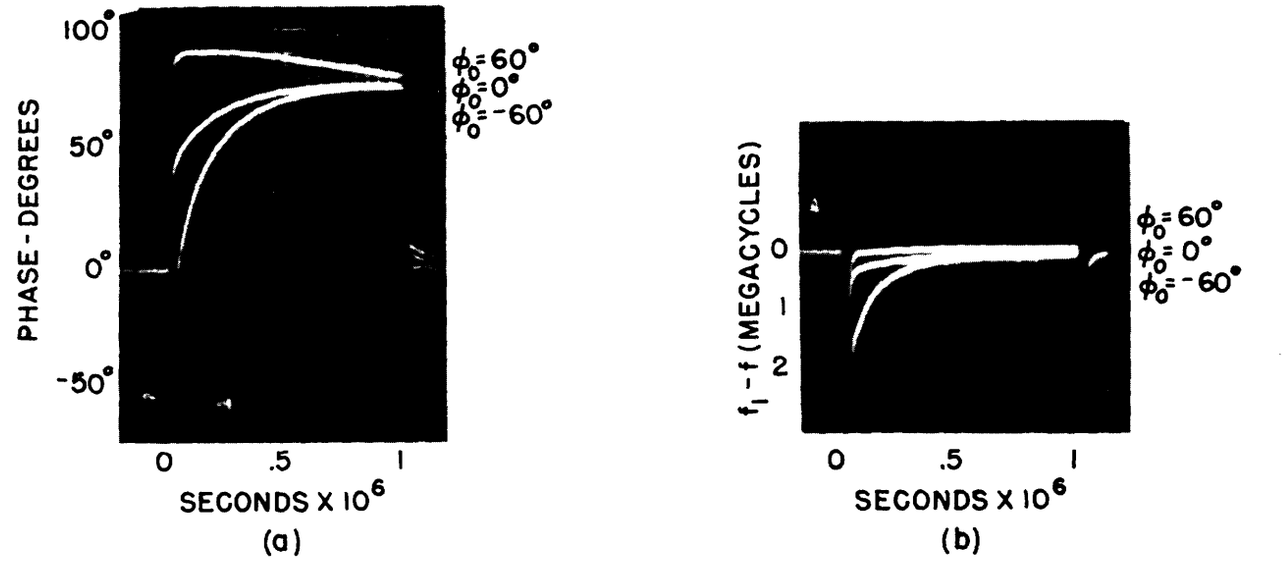

Fig 26 Phase and frequency for M/S = 0.95 showing the effect of changes in the initial condition.

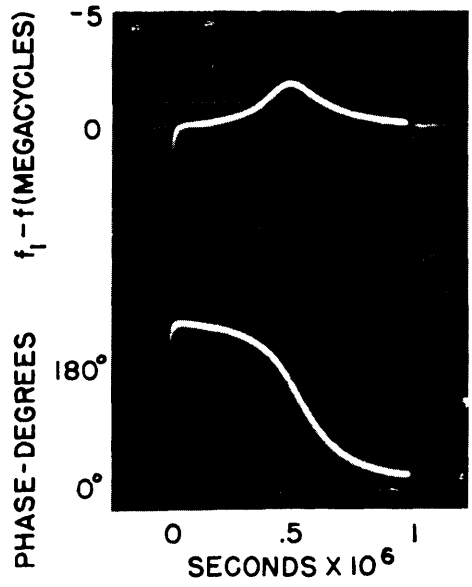

Fig. 27 Phase and frequency for M/S = 0.4 showing the effect of large positive initial angle.

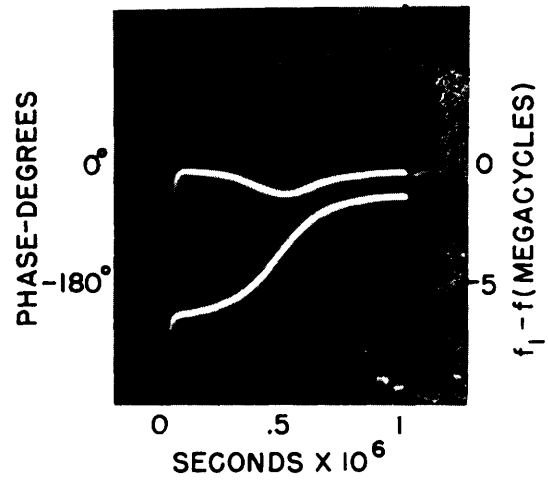

Fig. 28 Phase and frequency for M/S = 0.4 showing the effect of large negative initial angle.

Appendix I

It is possible to examine the equivalent load of a synchronized oscillator in an analytical manner. The resulting expression, together with the oscillator operating equation, allows the steady-state and transient behavior of the oscillator phase to be calculated. Assumptions involved in such a procedure make the result an approximation which is quite good when the synchronizing signal is small. This type of analysis has been applied to both triode and microwave oscillators. Portions of this particular solution are adapted from the work of J. C. Slater (7).

Consider a microwave oscillator whose voltage and current at its reference plane are $Ve^{j\omega t}$ and $ie^{j\omega t}$. Let there be an externally injected signal whose voltage and current at the oscillator reference plane are $V_1 e^{j\omega_1 t}$ and $i_1 e^{j\omega_1 t}$. If ω_1 and ω are not greatly different, the admittance presented to the oscillator at its plane of reference may be written

$$Y_L = \frac{ie^{j\omega t} + i_1 e^{j\omega_1 t}}{Ve^{j\omega t} + V_1 e^{j\omega_1 t}} \tag{I-1}$$

$$\text{or} \qquad Y_L = \frac{i}{V}\left[\frac{1 + \frac{i_1}{i} e^{j(\omega_1-\omega)t}}{1 + \frac{V_1}{V} e^{j(\omega_1-\omega)t}}\right] = (G + jB)\left[\frac{1 + \frac{i_1}{i} e^{j(\omega_1-\omega)t}}{1 + \frac{V_1}{V} e^{j(\omega_1-\omega)t}}\right] \tag{I-2}$$

where G + jB is the passive load admittance. If we carry out the indicated division and neglect all except the first two terms, Eq. (I-2) becomes

$$Y_L \simeq G + jB + 2\rho\, e^{j(\omega_1-\omega)t} \tag{I-3}$$

where $\rho = 1/2(i_1/i - V_1/V)(G + jB)$ and the approximation is good only when $V_1/V \ll 1$. Now ρ is known as the reflection factor and may be written

$$\rho = \frac{Y_{LP}}{2}\left(\frac{i_1}{i_i + i_r} - \frac{V_1}{V_i + V_r}\right) = \frac{Y_{LP}}{2}\left(-\frac{\rho_S}{1 - \rho_L} - \frac{\rho_S}{1 + \rho_L}\right)$$

$$\text{or} \qquad \rho = \frac{Y_{LP}\,\rho_S}{2}\left(\frac{2}{1 - \rho_L^2}\right) \simeq -\,Y_{LP}\,\rho_S \tag{I-4}$$

where we have separated the oscillator current and voltage into their incident and reflected components, $\rho_S = V_1/V_i = -\,i_1/i_i$ = reflection coefficient due to locking signal, and $\rho_L = V_r/V_i = -\,i_r/i_i$ = reflection coefficient due to passive load. Further, the approximation in Eq. (I-4) assumes that $|\rho_L|$ is less than about 0.3. Then the load admittance may be written approxi-

mately as

$$Y_L \simeq G + jB - 2|\rho|\ e^{j[(\omega_1-\omega)t+\phi]} \tag{I-5}$$

where ϕ is the phase of the reflection factor. Note that ϕ is the sum of the oscillator, locking signal, and load phases if the approximation in Eq. (I-4) is valid. In any case, the reflection factor phase is a linear function of the oscillator phase. Now we are particularly interested in the condition $\omega_1 = \omega$; that is, when the oscillator is synchronized. Incorporating this condition in Eq. (I-5), and substituting the resulting expression into the oscillator operating equation (1), we have after separation of the real and imaginary parts

$$\frac{g}{\omega_o C} = \frac{1}{Q_o} + \frac{G}{Q_{ext}} - \frac{2|\rho|}{Q_{ext}} \cos\phi \tag{I-6a}$$

$$\frac{b}{\omega_o C} \simeq 2\left(\frac{\omega_1 - \omega_o}{\omega_o}\right) + \frac{B}{Q_{ext}} - \frac{2|\rho|}{Q_{ext}} \sin\phi \quad . \tag{I-6b}$$

Equation (I-6b) is concerned with the oscillator frequency and phase, while Eq. (I-6a) specifies its power output. The former may be made to read

$$\frac{\omega - \omega'}{\omega_o} = \frac{|\rho|}{Q_{ext}} \sin\phi \tag{I-7}$$

where $\omega' = b/2C + \omega_o - \omega_o/2Q_{ext}\ B$, and is the frequency of oscillation in the absence of the locking signal. Then in the synchronized condition

$$\phi = \sin^{-1}\left[\frac{Q_{ext}\ (\omega_1 - \omega')}{|\rho|\omega_o}\right] \quad . \tag{I-8}$$

Now Eq. (I-7) may be written as a differential equation by allowing ω and ω_1 to differ, and noting that

$$\frac{d\phi}{dt} = \omega_1 - \omega \tag{I-9}$$

which permits us to write

$$\frac{d\phi}{dt} + \frac{|\rho|\omega_o}{Q_{ext}} \sin\phi = (\omega_1 - \omega') \quad . \tag{I-10}$$

This equation may be solved directly for ϕ as a function of time; its solution is (7)

$$\phi = \sin^{-1}\left[\frac{Q_{ext}\ (\omega_1 - \omega')}{|\rho|\omega_o}\right] + f(t) \tag{I-11}$$

where the condition $Q_{ext}\ (\omega_1 - \omega')/|\rho|\omega_o \leqslant 1$ must be satisfied. The

transient part of the solution indicated here by f(t) shows that when the locking signal is suddenly applied, the phase approaches its steady-state value in exponential fashion. The solution for

$$\frac{Q_{ext}(\omega_1 - \omega')}{|\rho|\omega_o} \gtrsim 1$$

reveals that Φ is a continuous function of time and, hence, locking is not accomplished for this condition.

Appendix II
((2)p. 493)

The equivalent circuit usually used to characterize a magnetron is shown in Fig. 29. Here the normalized load admittance, G + jB, is coupled to the operating mode, represented by R, C, and L. The factor K_C accounts for the transformer action of the coupling loop or iris, and g + jb is the non-linear admittance which characterizes the electronic discharge.

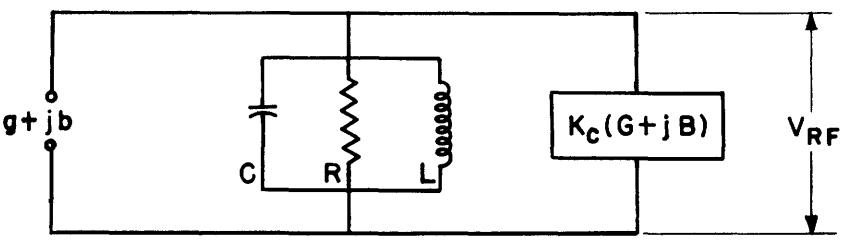

Fig. 29
Single mode equivalent circuit of a magnetron.

If the magnetron is operating in the steady-state, conservation of energy requires that the total admittance shunting any pair of terminals be zero. From this condition, we find the operating equations

$$\frac{g}{\omega_o C} = \frac{1}{Q_o} + \frac{G}{Q_{ext}}$$

$$\frac{b}{\omega_o C} = \left(\frac{\omega}{\omega_o} - \frac{\omega_o}{\omega}\right) + \frac{B}{Q_{ext}} \qquad \text{(II-1)}$$

where $\omega_o = 1/\sqrt{LC}$ = resonant mode frequency, $Q_o = R/\omega_o L = R\omega_o C$ = quality factor of the mode, and $Q_{ext} = \omega_o C/K_C = 1/K_C\omega_o L$ = loading effect of matched load. If the magnetron is in a transient condition, another term which accounts for energy storage in the mode must be added to the equations above. Specifically, the energy stored is

$$W = CV_{RF}^2 \qquad \text{(II-2)}$$

and the rate of energy storage is

$$\frac{dW}{dt} = 2CV_{RF}\frac{dV_{RF}}{dt} \quad . \tag{II-3}$$

At any instant this rate may be represented as a conductance shunting the circuit of Fig. 29. The magnitude of this shunting effect is

$$G_S V_{RF}^2 = 2CV_{RF}\frac{dV_{RF}}{dt}$$

or

$$G_S = \frac{2C}{V_{RF}}\frac{dV_{RF}}{dt} \tag{II-4}$$

so that Eq. (II-1) becomes

$$\frac{g}{\omega_o C} = \frac{1}{Q_o} + \frac{G}{Q_{ext}} + \frac{2}{\omega_o}\frac{1}{V_{RF}}\frac{dV_{RF}}{dt} \tag{II-5a}$$

$$\frac{b}{\omega_o C} = \left(\frac{\omega}{\omega_o} - \frac{\omega_o}{\omega}\right) + \frac{B}{Q_{ext}} \quad . \tag{II-5b}$$

Now if g is known as a function of V_{RF}, then Eq. (II-5a) may be solved to find V_{RF} as a function of time. Assuming the empirical relation

$$g = \frac{E/R}{V_{RF}} - \frac{1}{R} \tag{II-6}$$

we find

$$V_{RF} = \frac{E}{RC\omega_o}\frac{1}{\left(\frac{1}{RC\omega_o} + \frac{1}{Q_L}\right)}\left\{1 - e^{-\frac{\omega_o}{2}\left(\frac{1}{RC\omega_o} + \frac{1}{Q_L}\right)t}\right\}$$

$$V_{RF} = V_{RF_o}\left(1 - e^{-kt}\right) \tag{II-7}$$

where $V_{RF_o} = \frac{E}{RC\omega_o}\frac{1}{\left(\frac{1}{RC\omega_o} + \frac{1}{Q_L}\right)}$, $k = \frac{\omega_o}{2}\left(\frac{1}{RC\omega_o} + \frac{1}{Q_L}\right)$, and $\frac{1}{Q_L} = \frac{1}{Q_o} + \frac{1}{Q_{ext}}$.

Now in the derivation of Eq. (70) we found that the coefficient N was

$$N = \frac{E\eta}{2CRV_{RF_o}}\tan\alpha \quad . \tag{II-8}$$

If we substitute our expression for V_{RF_o}, we find

$$N = \frac{\omega_o}{2}\left(\frac{1}{RC\omega_o} + \frac{1}{Q_L}\right)\eta\tan\alpha = k\eta\tan\alpha \quad . \tag{II-9}$$

ACKNOWLEDGMENT

The author gratefully acknowledges the encouragement and many helpful suggestions of Professors J. B. Wiesner and J. C. Slater, Dr. A. B. Macnee, Dr. R. B. Adler, and Mr. L. D. Smullin during the course of this research.

BIBLIOGRAPHY

(1) E. E. David, Jr., Locking phenomena in microwave oscillators, R.L.E. Technical Report No. 63, M.I.T. (April 8, 1948).

(2) J. C. Slater, Microwave electronics, Rev. Mod. Phys., 18, 441-512 (Oct., 1946).

(3) S. Goldman, Frequency analysis, modulation, and noise, McGraw-Hill Co., New York (1948).

(4) J. C. Slater, The operation of magnetrons, R.L. Report No. 43-28, M.I.T. (1943).

(5) G. B. Collins, Microwave magnetrons, R.L. Series No. 6, McGraw-Hill Co., New York (1948).

(6) A. B. Macnee, An electronic differential analyzer, R.L.E. Technical Report No. 90, M.I.T. (Dec. 10, 1948).

(7) J. C. Slater, The phasing of magnetrons, R.L.E. Technical Report No. 35, M.I.T. (April 3, 1947).

(8) J. H. Vincent, On some experiments in which two neighboring maintained oscillatory circuits affect a resonating circuit, Proc. Phys. Soc., 32, 84-91 (1919-1920).

(9) E. V. Appleton, The automatic synchronization of triode oscillators, Proc. Camb. Phil. Soc., 21, 231-48 (1922-1923).

(10) B. Van der Pol and H. V. Appleton, On the form of free triode vibrations, Phil. Mag., 6-42, 201 (Aug. 1921).

(11) B. Van der Pol, Forced oscillations in a circuit with non-linear resistance, Phil. Mag., 7-3, 65 (Jan. 1927).

(12) H. S. Möller, Uber Störungsfreien Gleichstromempfang mit den Schwingaudion, Jahr. für Draht. Teleg., 17, 256-87 (April, 1921).

(13) S. Byard and W. H. Eccles, The locked-in oscillator, Wireless Eng., 18, 2-6 (Jan. 1941).

(14) C. W. Carnahan and W. P. Kalmus, Synchronized oscillators as frequency-modulation receiver limiters, Electronics, 17, 108-12 (Aug., 1944).

(15) G. L. Beers, A frequency-dividing locked-in oscillator frequency-modulation receiver, Proc. I.R.E., 32, 730-38 (Dec., 1944); Elect. Eng. (Dec., 1944).

(16) D. G. Tucker, The synchronization of oscillators, Elect. Eng., 15, 412-18 (March, 1943); 457-61 (April, 1943); 16, 26-30 (June, 1943).

(17) D. G. Tucker, Forced oscillations in oscillator circuits, Jour. I.E.E. (London), 92, 226-34 (Sept., 1945).

(18) R. Adler, A study of locking phenomena in oscillators, Proc. I.R.E., 34, 351-57 (June, 1946).

(19) R. D. Huntoon and A. Weiss, Synchronization of oscillators, Proc. I.R.E., 35, 1415-23 (Dec., 1947).

* * *